Departement für Pferde, Klinik für Pferdechirurgie
der Vetsuisse-Fakultät Universität Zürich

Direktor: Prof. Dr. med. vet. Anton Fürst, Dipl. ECVS

Arbeit unter wissenschaftlicher Betreuung von
Dr. med. vet. Stephan Zeiter, PhD, Dipl. ECLAM

Does the sorting of mesenchymal stem cells based on their Runx2/Sox9 expression ratio improve bone healing in calvarial defects in rats?

Inaugural-Dissertation

zur Erlangung der Doktorwürde der
Vetsuisse-Fakultät Universität Zürich

vorgelegt von

Fabian Gieling

Tierarzt
von Steinheim, Deutschland

genehmigt auf Antrag von

Prof. Dr. med. vet. Anton Fürst, Referent
Prof. Martin J. Stoddart, PhD, Korreferent

2017

Für meine Familie

Contents

1 Summaries

1.1 Abstract

Mesenchymal stem cells have been investigated as an alternative source of osteogenic cells for the repair of large bone defects. Previously, a more homogeneous population of human mesenchymal stem cells (hMSCs) was identified that showed enhanced osteogenic potential *in vitro*. The cells were isolated by the relative expression of Runx2 compared to Sox9. In this study, it was investigated if these sorted cells based on their Runx2/Sox9 ratio can improve bone healing *in vivo* in a nude rat calvarial defect model.

Five millimeter bone defects were generated and filled with either sorted or unsorted cells, both seeded on a collagen membrane, or with the membrane only. In vivo CT analysis was carried out post OP, 2 weeks after surgery and after euthanasia 4 weeks post OP to show bone ingrowth into the defect. The fluorochrome Xylenol Orange was used for labeling bone formation after 3 weeks and all samples were analyzed histologically for bone formation and inflammation.

Neither the CT nor the histological results led to a statistically significant difference between the 3 groups, but the control group (membrane only) trended towards producing the most new bone, especially after 2 weeks. This may suggest that the seeded cells impair bone healing. A possible reason for this could be a rejection triggered in response to the hMSCs, despite the lack of T cells in nude rats. Further studies are needed to identify the reasons.

1.2 Zusammenfassung

Mesenchymale Stammzellen werden als alternative Quelle für osteogene Zellen zur Reparatur großer Knochendefekte untersucht. Aktuell wurde eine homogenere Population von humanen mesenchymalen Stammzellen (hMSCs) identifiziert, die *in vitro* ein erhöhtes osteogenes Potential zeigten. Die Zellen wurden durch die relative Expression von Runx2 im Vergleich zu Sox9 isoliert. In dieser Studie wurde untersucht, ob diese nach ihrem Runx2/Sox9-Verhältnis sortierten Zellen die Knochenheilung *in vivo* in einem Schädelkalottendefektmodell in Nacktratten verbessern können.

Fünf Millimeter Knochendefekte wurden mit sortierten oder unsortierten Zellen, jeweils auf einer Kollagenmembran gesät oder nur mit der Membran gefüllt. Die Knochenbildung im Defekt wurde mit CT Aufnahmen post OP, nach 2 Wochen und nach Euthanasie 4 Wochen post OP dargestellt. Das Fluorochrom Xylenolorange wurde zur Markierung der Knochenbildung nach 3 Wochen verwendet. Histologisch wurde die Knochenbildung und Entzündung analysiert.

Weder in der CT-Analyse noch in der Histologie wurde zwischen den 3 Gruppen ein statistisch signifikanter Unterschied beobachtet, jedoch schien die Gruppe mit nur der Membran v.a. nach 2 Wochen tendenziell mehr Knochen zu bilden. Dies könnte darauf hindeuten, dass die Anwesenheit von Zellen die Knochenheilung beeinträchtigen. Ein möglicher Grund dafür könnte eine Abstossungsreaktion auf die hMSCs sein, trotz des T-Zell Mangels in Nacktratten. Weitere Studien sind zur Ermittlung der Gründe nötig.

2 Introduction

2.1 Clinical problem

Serious high-energy accidents, resections of bone tumors or cysts, revision surgeries of non-healing fractures (nonunion), joint implant loosening and the treatment of bone infections can lead to large bone defects whose treatment is often complicated and difficult.[1]

More than two million bone grafting procedures are carried out worldwide annually.[2]

A bone graft with autologous bone is still the gold standard for the repair of large bone defects.[3] The advantage of this method is that the filling material has all the important properties for bone regeneration, since autologous bone graft is both osteoconductive and osteoinductive and also contains osteogenic cells therefore representing the ideal treatment.[3–5]

However, the amount of autologous bone available is limited and the complication rate (blood loss, hematoma formation, infections, pain at the removal site) is up to 20%.[6, 7]

2.2 Bone-graft substitutes

Bone-graft substitutes can either be used in place of an autograft or expand the existing amount of an autologous bone graft.[5, 8] Kolk *et al* described the ideal bone graft substitute as biocompatible, bioresorbable, osteoconductive, osteoinductive, structurally similar to bone, easy to use and cost-effective.[3] Bone graft substitutes are known as important alternatives to bone grafting in dental surgery, implantology and periodontology.[3] As an alternative to autologous bone, allogeneic (from same species) or even xenogeneic (from a different species) bone can be used. Nevertheless, there is a risk of a rejection reaction or transmission of diseases (HIV, zoonosis, etc.). Due to these limitations, new bone graft substitutes are being investigated, which have unlimited availability, are inexpensive and have similar characteristics as autologous bone grafts.

Nandi *et al* [8] modified the Laurencin *et al* [9] classification of grafts and graft substitutes as shown in this overview:

Table 1: Bone grafts and graft substitutes

Class	Description	Examples
Autograft based	Used alone or in combination with other materials	Bone autografts Autologous bone marrow
Allograft based	Used alone or in combination with other materials	Bone allografts Allogenic bone marrow Demineralized bone matrix (DBM)
Factor based	Natural and recombinant growth factors used alone or in combination with other materials	Transforming growth factor beta (TGFβ) Basic fibroblast growth factor (bFGF) Platelet derived growth factor (PDGF) Bone morphogenetic proteins (BMPs) Insulin like growth factor (IGF-1) Vascular endothelial growth factor (VEGF)
Cell based	Cells to generate new tissue alone or seeded onto a support matrix	Mesenchymal stem cells Collagen Gene therapy
Ceramic based	Used alone or in combination with other materials	Calcium phosphate cement Calcium sulfate Calcium hydroxyapatite (HAp) Tri-calcium phosphate (TCP) Bioactive glass
Polymer based	Degradable and nondegradable polymers	Open porosity polylactic acid polymer (OPLA)
Miscellaneous	Various marine biomaterials	Coral Chitosan

In this study, cell-based bone graft substitutes were investigated focusing on the potential of stem cells to improve bone healing.

2.3 Stem cells

Stem cells are cells of different origins with a high self-renewal capacity [10] and can be divided into two groups: embryonic stem cells (ESCs) and non-embryonic adult or somatic stem cells.[11, 12]

ESCs are pluripotent cells and can be isolated from the inner cell mass of a blastocyst. This leads to the destruction of the blastocyst and causes ethical issues.[13]

Adult stem cells are multipotent cells and can be divided into two populations: hematopoietic stem cells and mesenchymal stem cells (MSCs).[11] Such MSCs can be isolated from bone marrow aspirates known as bone marrow stromal stem cells (BMSCs).

Mesenchymal stem cells have a high potential for proliferation and differentiation. The activation or suppression of genes allows their differentiation to be actively controlled. They can differentiate into different cell types for example osteogenic, chondrogenic or adipogenic cells. It has been shown that MSCs are involved in intramembranous ossification and can differentiate into osteoblasts.[14] Therefore, mesenchymal stem cells are regarded as a source of osteogenic cells, but their use in the clinic has not yet been established. In part, this can be explained by the fact that mesenchymal stem cells represent a very inhomogeneous cell population, which can, in turn, lead to varying efficacy as osteogenic cells.

Recent *in vitro* studies demonstrated that the osteogenic differentiation of human bone marrow mesenchymal stem cells depends on the ratio of two important transcription factors: Runx2 and Sox9.[15–17] Neither Runx2 nor Sox9 is a specific marker for osteogenesis. Runx2 is known as an important transcription factor expressed in MSCs for their osteogenic differentiation.[18] Sox9 is involved in chondrogenic differentiation, but Loebel *et al* showed that Sox9 also plays a major role in the regulation of osteogenesis by interacting with Runx2 by repressing its activity. Thus, the Runx2 / Sox9 ratio has been recommended to describe the

osteogenicity of human MSCs. This has been proposed as a promising early screening method.[15, 18]

Smart-Flare™ probes can detect mRNA using nanoparticle probes (Figure 1). The probes consist of two different strands attached to gold nanoparticles. One strand is a capture oligonucleotide specific for the gene of interest. The other strand is a fluorescently labelled short oligonucleotide. When complimentary RNA is present, the fluorescently labelled short oligonucleotide leaves the gold nanoparticle and fluoresces. These cells can be used afterwards for further investigations or therapies.[15, 19] Li *et al* used this method to observe mRNA expression of Runx2 and Sox9 in living cells at the individual cell level.[15]

Smart-Flare™ probes for Runx2 Cy3 and Sox9 Cy5 were used to prospectively identify a more homogenous population of hBMSCs by sorting the isolated cells with fluorescence activated cell sorting (FACS). In a second step a mineralization assay was used to further investigate the isolated cell population. A fraction with an increased osteogenic differentiation potential and a decreased proliferation rate was identified. These sorted, more homogeneous cells showed an improved osteogenic potential when compared to unsorted heterogeneous cells in vitro.[15] Thus these sorted cells could be a clinically relevant source of cells for improved healing of bone defects.

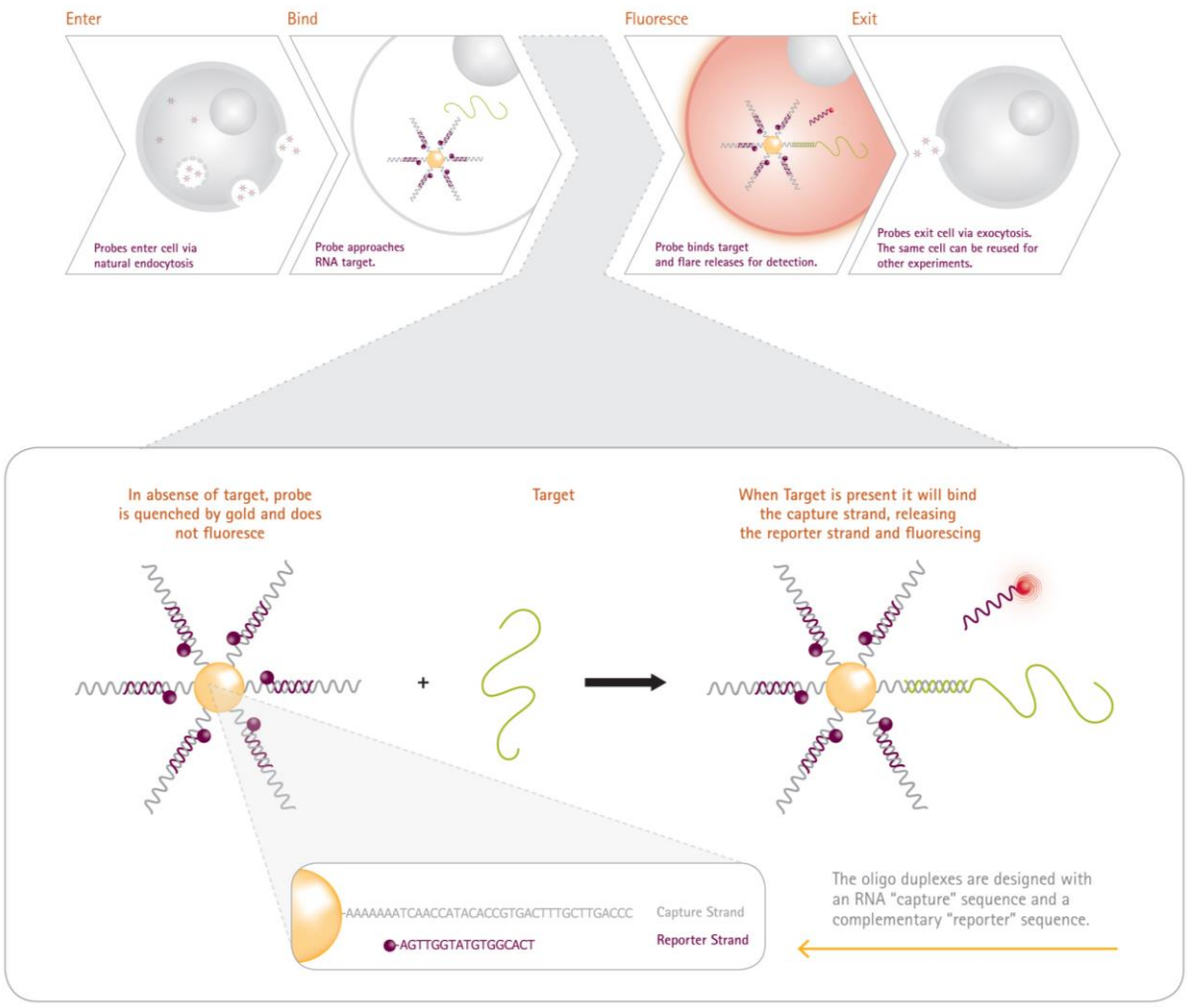

Figure 1: The SmartFlare™ probe's simple mechanism reveals the RNA content of live cells while keeping cells alive and intact. SmartFlare™ probes enter the cell using the cells's own endocytosis process. The probes circulate within the cell and bind to the complementary RNA sequence. This binding event releases a fluorophore, illuminating the cells for detection. Over time, the probe exits the cell, leaving the cell unchanged and free for downstream analyses. (Figure and text kindly provided by Merck KGaA Darmstadt)

2.4 Hypothesis

Within the scope of this "proof of concept" study the goal was to confirm these *in vitro* results *in vivo*. The sorted and thus more homogeneous cell population was compared with the unsorted cell population. The hypothesis was that hBMSCs sorted based on their Runx2 to Sox9 ratio lead to more newly formed bone within the first four weeks after defect creation surgery than unsorted cells in calvarial defects in nude rats.

3 Materials and methods

3.1 Study Design

All procedures were carried out in an AAALAC (Association for Assessment and Accreditation of Laboratory Animal Care) accredited and GLP (Good Laboratory Practice) certified facility according to the Swiss Laws of animal welfare. The animal experiments were approved by the Animal Welfare Commission of the official veterinary authorities (Authorization Number GR 33_2016).

Twelve female RNU (Crl:NIH-Foxn1rnu) nude rats (13 to 17 weeks-old), purchased from Charles River Laboratories, Germany, were enrolled in this study. Each received two five millimeter calvarial bone defects. The calvarial defect serves as a model for intramembranous bone formation.[20, 21] Since the isolated cells are more osteoblastic in nature, this intramembranous calvarial model was used. Five mm defects are reported to be subcritical [20] or critical defects. [22, 23]

RNU nude rats were chosen in order to avoid an immune reaction to the human mesenchymal stem cells (hBMSCs) which were used in this study. They are athymic and T-cell deficient and show depleted cell populations in thymus-dependent areas of peripheral lymphoid organs.[24]

The defects were systematically randomized between three groups according to Table 2. They were filled with a collagen membrane which contained either sorted hBMSCs based on the ratio of the two transcription factors Runx2 and Sox9 (group A), unsorted human mesenchymal stem cells (group B) or, as a control, the collagen membrane contained no cells (group C). The collagen membrane was a collagen type I cell carrier for 96-Well Plates purchased from Viscofan BioEngineering, Germany.

Table 2: Groups

Group	Description
A	Cells sorted on their Runx2/Sox9 ratio seeded on collagen membrane
B	Unsorted cells seeded on collagen membrane
C	Collagen membrane only

The primary goal of this study was to assess the bone healing. Micro computed tomography (CT) and histology was used. The rats were scanned in a micro CT postoperatively, two weeks after surgery and after euthanasia to follow the progress of healing. Bone volume and density at each time point as well as bone evolution over time was evaluated (see Figure 2).

After euthanasia a histological examination for bone formation and inflammation with microscopic evaluation and epifluoroscopic analysis followed. The fluorochrome Xylenol Orange was injected subcutaneously three weeks after the defect surgery to visualize bone formation and bone remodeling at this time point. The investigators were blinded at the time of the histological examination.

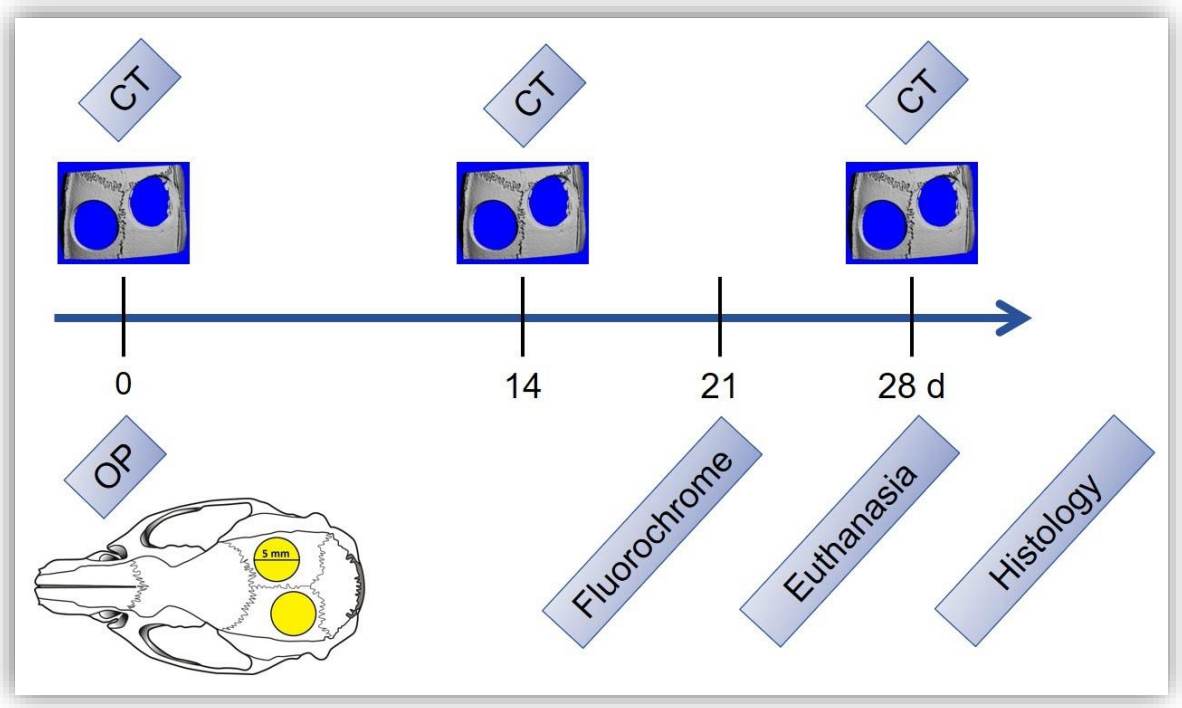

Figure 2: Timeline

3.2 Animals

3.2.1 Inclusion criteria and preoperative care

Specific pathogen free (SPF) female RNU (Crl:NIH-Foxn1rnu) nude rats were purchased from Charles River Laboratories, Germany. They were acclimatized for five to nine weeks before the start of the study. The inclusion criteria were defined as an age of twelve to 18 weeks with a weight of 150 to 250 grams before the surgery. All rats had to have a health certificate from the breeder and to be judged clinically healthy based on a preanesthetic clinical examination by a veterinarian.

To prevent eye problems due to the missing eyelashes of nude rats, the eyes were cleaned two times a week with sterile Ringer's solution (B. Braun Melsungen AG, Germany) and sterile swabs (IVF Hartmann AG, Switzerland).

3.2.2 Housing and feeding

Up to four rats per cage were group housed in individually ventilated cages (IVC, Type 2000 Rat Cage, Allentown Inc, United States) with an area of 2000 cm^2 and a height of 26 cm with a 12:12 hours light:dark cycle and bedded on laboratory wood bedding (ABEDD Vertriebs GmbH, Austria). All procedures with the animals were performed in a laminar flow work station (Phantom Animal Transfer Station, Allentown Inc, United States). Room temperature was maintained at 22 ± 2 °C with a relative humidity of 40-60 %. In the background, a radio (<80 dB) ran in order to accustomize the animals to noise and to prevent stress due to a suddenly rising noise level (e.g. feeding, cage changes).

As an enrichment material, the rats were given paper, a cardboard house and wood for gnawing on.

The rats were fed ad libitum a commercial pelleted diet food (KLIBA NAFAG, PROVIMI KLIBA AG, Switzerland: "mouse and rat maintenance" Extrudate 15 mm round). They were offered water ad libitum at all times.

In the week before the operation the rats were offered a nutritional gel (MediGel® Sucralose, ClearH2O, Bio Services, The Netherlands) in the cage so that they could get used to this nutritional gel which served as a carrier gel after surgery for administration of carprofen medications.

3.2.3 Health monitoring

Samples of three different locations (body swab, oral swab, fecal pellets; all samples from the same location from all animals were pooled) for a Rat Surveillance PRIA (PCR Rodent Infectious Agent) Test were collected two weeks before surgery and just before euthanasia to gain an overview of the health status and to identify viral, bacterial, fungal and parasitic agents in the animals. This special health monitoring test is based on PCR assays and is available for different pathogens (for a list of all agents see Attachments).[25] The samples were analyzed by Charles River Research Animal Diagnostic Services, Wilmington, USA.

3.3 Cells and membrane

A Collagen Type I Cell Carrier, Ø seven mm from Viscofan BioEngineering, Weinheim, Germany was used in the study. These membranes are 20 µm thin based on fibrillar, bovine collagen I and chemically non-crosslinked. They were trimmed to five mm diameter using a sterile biopsy punch (kai medical, kai Europe GmbH, Solingen, Germany).

Bone marrow was harvested from the femoral head from a 91 year old male human (Ethical approval: Freiburg, EK-326/08) and diluted 1:4 with phosphate buffered saline (PBS, Sigma-Aldrich Chemie GmbH, Switzerland). The mixture was carefully layered on a Ficoll cushion (Histopaque-1077, Sigma-Aldrich Chemie GmbH, Switzerland), and centrifuged at 800× g for 20 minutes. The mononuclear cells were collected from the liquid interface. To exclude red blood cells a gated cell count was performed using a cell Scepter 2.0 Automated Cell Counter (Millipore, Germany). Isolated mononuclear cells were seeded at a density of 50,000 cells/cm^2 in cell culture flasks, and cultured in α -modified essential medium (α -MEM; GIBCO, Switzerland), 10% fetal bovine serum (Sera Plus, PAN-Biotec, Germany), 1% penicillin and streptomycin (GIBCO, Switzerland), and 5 ng/ml recombinant human basic fibroblast growth factor (bFGF, Fitzgerald Industries International, USA). Nonadherent hematopoietic cells were removed after four days. Cells were incubated at 37 °C and 5% CO_2 and the medium was refreshed every second day. Cell surface marker profiling was performed at passage one according to previous protocols.[26] The potency of the expanded attached cells to differentiate towards chondrogenic, osteogenic and adipogenic lineages was confirmed.[15]

Passaged hBMSCs were cultured in a growth medium which contains α -modified essential medium (α -MEM; GIBCO, Switzerland), 10% fetal bovine serum (Sera Plus, PAN-Biotec, Germany), 5 ng/ml recombinant human basic fibroblast growth factor (bFGF) and 1% penicillin and streptomycin (GIBCO, Switzerland) for one week to achieve the desired number of cells with an initial seeding density of about 3000/cm^2. Normal growth medium allows proliferation of the cells but no differentiation.

hBMSC foreseen for group A were induced with osteogenic induction medium which contains Dulbecco´s modified Eagle’s medium low glucose (DMEM; GIBCO,

Switzerland), 10% fetal bovine serum (Sera Plus, PAN-Biotec, Germany), 1% penicillin and streptomycin (GIBCO, Switzerland), 50 µ g/ml ascorbic acid, 10 nM dexamethasone and 5 mM β -glycerol phosphate (Sigma-Aldrich, Switzerland) for one week. Osteogenic induction medium allows differentiation of the cells. These cells were sorted using flow cytometry (BD Aria III, BD Biosciences, Switzerland) based on their Runx2/Sox9 ratio as described by Li *et al* [15]. Therefore, SmartFlare™ probes for Runx2 and Sox9 were added to the medium and incubated at 37°C and 5% CO_2 overnight. To detach the cells after 16 hours 0.05% Trypsin-EDTA (GIBCO, Switzerland) was used. The cells were centrifuged at 2000 rpm for 10 min. and the cell pellet was resuspended in growth medium afterwards. Finally the cells were analyzed based on their fluorescence intensity by FACS and sorted into four populations. The population with a low Sox9 and a low Runx2 fluorescence intensity (P1 population as characterized by Li *et al* [15]) was selected to be used in this study. This population showed in vitro the highest osteogenic differentiation potential and lowest proliferation rate. This corresponds most closely to the properties of osteoblasts.[15]

hBMSCs foreseen for group B (no sorting) were cultured in growth medium for two weeks. These cells were not induced with osteogenic induction medium.

Two days prior to surgery the cells of all groups were seeded on the membrane to allow cell attachment and were cultured in growth medium. Before seeding, membranes were first attached on the plate (96 well plate) overnight according to the manufacturer's instructions. The cells were seeded on the upper side of the membrane and they were implanted in the animal so that the cells were on the top.

Cell number was constant at 375,000 per membrane. The exact number was determined at the time of seeding.

Membranes for group C were also placed in 96 well plates with the same growth medium two days prior to surgery.

3.4 Surgical Intervention

3.4.1 Anesthesia & Analgesia protocol

The surgery was performed under general anesthesia. Inhalation agents were preferred for this study because of their controllability. Sevoflurane (Sevoflurane Baxter®, Baxter AG, Switzerland) was used in oxygen in a non-rebreathing anesthesia system. The animals were placed in an induction box with oxygen (1l/min) and 5-6% sevoflurane.

When the animal was recumbent and the righting reflex was absent the animal was taken out of box and the animals head was placed in the face mask. The vaporizer setting was reduced to 2-3% sevoflurane and the oxygen flow to 0.6-1.0 l/min. Eye lube was applied in both eyes (Vitamin A Blache Augensalbe, Bausch und Lomb Swiss AG, Switzerland) to prevent drying of the cornea.

During the preparation and surgery, the respiratory rate was monitored by an experienced anesthetist and the animals were placed on a heating pad to maintain core temperature. The temperature was measured rectally before surgery and after CT.

Preoperative analgesia: Preoperatively, buprenorphine (Bupac®, Streuli Pharma AG, Switzerland, 0.01 mg/kg, subcutaneously) and carprofen (Norocarp®, ufamed AG, Switzerland, 5 mg/kg, subcutaneously) were given to the rats for pain management.

Intraoperative analgesia: Ropivacaine 2 mg/ml (ROPIVACAIN Fresenius, Fresenius Kabi, Switzerland, 3 mg/kg) was dropped onto the periosteum after cutting the skin.

Postoperative analgesia: The rats were injected with buprenorphine (Bupac®, Streuli Pharma AG, Switzerland, 0.01 mg/kg, subcutaneously) 4-6 h and 9-11 h after surgery and the next morning. Additionally, the animals received carprofen (5 mg/kg) in a nutritional gel (MediGel® CPF, ClearH2O, Bio Services, The Netherlands) oral for the first three days post-surgery.

The animals received two Milliliters of warm lactated Ringer's solution (B. Braun Medical AG, Switzerland) subcutaneously at the end of surgery to prevent dehydration of the animals.

All substances, their manufacturers, dose rates and routes and intervals of administration are listed in the table below.

Table 3: Used drugs during study

Purpose	*Substance*	*Registered trade name / Swiss manufacturer / Swissmedic no.*	*Dose and route of administration*
Induction and Maintenance of general anesthesia	Sevoflurane	Sevoflurane Baxter® / Baxter AG / 57671	2-3% Sevoflurane in oxygen 0.6-1 L/min
Pre-operative analgesia	Buprenorphine	Bupac® / Streuli Pharma AG / 63081	0.01 mg/kg s.c.
	Carprofen	Norocarp® / ufamed AG / 60459	5 mg/kg s.c.
Local anesthesia	Ropivacaine 2 mg/ml	ROPIVACAIN Fresenius / Fresenius Kabi AG / 61877	3 mg/kg s.c.
Post-operative analgesia	Buprenorphine	as above	0.01 mg/kg s.c. 4-6 h and 9-11 h after surgery and the next morning
	Carprofen	MediGel® CPF / Clear H2O	5 mg/kg oral for 3 days

3.4.2 Surgical procedure

The animal was placed in sternal recumbency, the head was clipped and aseptically prepared with diluted Betadine solution (Mundipharma Medical Company, Switzerland) followed by a rinse with sterile Ringer's solution (B. Braun Melsungen AG, Germany). The rats were draped with sterile incise-drapes (DYNJSD1021,

Medline, USA) on a sterile covered table (8371CEB, Medline, USA). A straight skin incision down to periosteum was made over the scalp sagittaly from the nasal bone to the occipital bone (Figure 3). 0.3 ml of Ropivacain (2 mg/ml, Fresenius Kabi AG, Switzerland) was dripped on the periosteum. After three minutes waiting period the periosteum was sharply divided in the midline and then gently pushed laterally.

In the area of the parietal bones, two evenly distributed five mm diameter craniotomy defects were prepared, one on each side of the sagittal suture (Figure 4), with a five mm Diamond-Trephine (JMP Dental GmbH, Germany, Art. No. DD229040) and a dental handpiece under constant irrigation with sterile Ringer's solution (B. Braun Melsungen AG, Germany) to prevent overheating. Initially the hole was pre-drilled with the trephine only. Then a custom-made metal ring was screwed on the trephine to limit the drill depth to less than one millimeter (Figure 5). A preliminary study on skulls of rat cadavers revealed a calvarian bone thickness of around 0.5 mm. The bone was not entirely penetrated by the trephine. The trephine was only used gradually until the bone was perforated at one point and the dura mater became visible. To assure the preservation of the dura mater a small blunt periosteal elevator was then used to remove the bone from the defect (Figure 6). Care was taken to avoid injury to the dura mater. Any damage to the dura mater was recorded on the surgery report.

Subsequently, the surgical area was thoroughly flushed with sterile Ringer's solution (B. Braun Melsungen AG, Germany) to remove bone debris. The two defects were filled with the materials to be tested according to Table 10 (see Attachments). The membranes were sized to fit exactly into the defects and were positioned on the dura mater but not secured. They were placed in a way that the seeded cells were located on the upper side of the membrane. Wound closure was performed in a two-layer technique: fascia single interrupted sutures (Vicryl rapid 5-0, Ethicon, Johnson & Johnson Medical, Switzerland) and skin in a continuous suture pattern intracutaneously (Vicryl rapid 5-0, Ethicon, Johnson & Johnson Medical, Switzerland).

The preparation of the animal and the surgery were carried out under a laminar air flow in the surgical theatre.

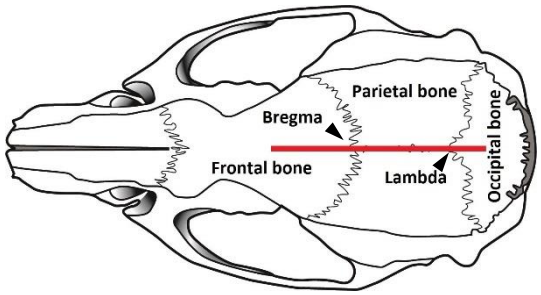

Figure 3: Position of skin incision (red line); rostral shown at left side, caudal at right side.

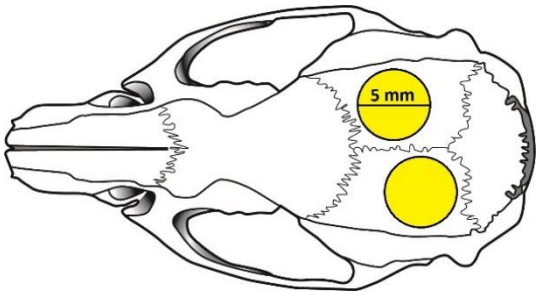

Figure 4: Position of the two defects in the calvaria; rostral shown at left side, caudal at right side.

A

B

Figure 5: A: Five mm Diamond-Trephine (JMP Dental GmbH, Germany, Art. No. DD229040), B: Trephine with custom-made metal ring to limit drilling depth

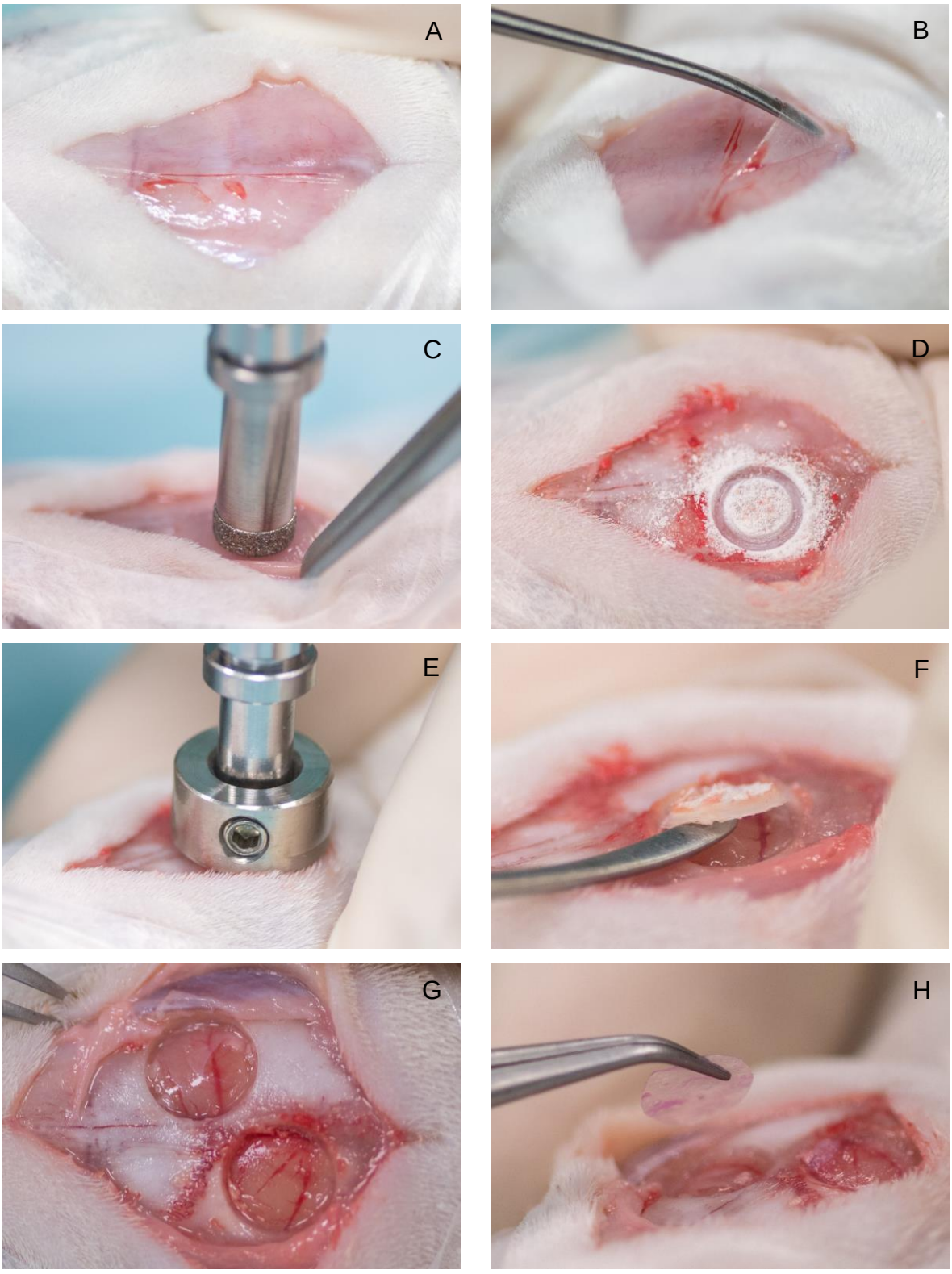

Figure 6: Creation of the defect shown on a cadaver, rostral is always left: Skin incision (A). Sharp incision of the periosteum in the midline and gentle removal to laterally (B). Pre-drilling of the defect with trephine only (C, D). Final drilling with a metal ring screwed on for depth control (E). Removal of the bone from the defect with a small blunt periosteal elevator (F). Defects with the exposed dura mater and brain shimmering through (G). Placement of the membrane into the defect (H).

3.4.3 Postoperative care

After surgery, the rats were directly transferred into the CT holder (see 3.6.3 Micro computed tomography), imaged, then taken out of the CT holder and placed in a recovery cage.

During the recovery phase, all animal stayed under the supervision of a veterinarian until fully awake and return of righting reflex. To prevent hypothermia a heating pad was placed under the cage and infrared light above the cage.

3.5 Animal welfare assessment

To guarantee an objective assessment of the postoperative animal welfare a predefined score sheet was used (Figure 7). The rats were scored twice a day for the first 3 days postoperatively, and daily thereafter for the first 7 days after surgery. Afterwards they were scored weekly. The scoring was performed by veterinarians and qualified animal caregivers.

This scoring was based on behavior, appearance of skin, fur and eyes, hang of the head, breathing, wound healing, weight loss and feces. It defined abruption criteria and actions to be taken depending on the achieved score (Figure 8): A veterinarian had to examine each animal that reached a score of more than three. He could adapt the treatment plan (for example he could administer additional analgesia) and had to decide if the scoring frequency had to be intensified.

Abruption criteria were defined as a score higher or equal to six for three days or a single score of equal or more than ten to avoid a high burden of the animal. Further any incident, which influence the study results (for example infections or diseases unrelated to the study) led to exclusion of the animal from the study.

Behavior/habitude	
- quiet and attentive	0
- huddled/inactive OR hyperactive	2
- apathetic= no reaction to stimulus	4
Appearance (fur, eyes, skin)	
- normal	0
- little dirty, sticky, scrubby fur	1
- very dirty, sticky, loss of fur	3
Head position	
- normal, head straight	0
- partial head tilt	1
- constant head tilt	2
- head tilt, neurological symptoms	3
Breathing	
- normal	0
- increased frequency	2
- very intensive	3
Wound healing	
- normal	0
- signs of inflammation (swelling, reddening, temperature ↑)	1
- signs of infection (secretion, + signs of inflammation ↑)	3
Surgery weight	0
- loss of 1 - 10% to surgery weight	1
- loss of 11 - 20% to surgery weight	3
- loss of > 20% to surgery weight	4
Feces/urine	
- normal	0
- abnormal (consistency, amount, color)	2
Total	
Signature	

Figure 7: Score sheet

Score	Reaction
0 to 3	no to moderate disturbance/suffering
4 to 9	moderate pain/suffering → increase observation interval, drugs
≥10	severe pain/suffering → consider abruption criteria → euthanasia
Group housing: if score ≠ 0 → examine individual rat	
if score more than 3 days ≥6 → consider abruption criteria → euthanasia	

Figure 8: Measures to be taken depending on score

3.6 In vivo analysis

3.6.1 Body weight

The body weight was measured at surgery, three and seven days after surgery, weekly thereafter and at euthanasia.

3.6.2 White blood cell count

Before surgery, at two weeks before the CT scan and before euthanasia 100-200µl blood from the tail vein was collected in EDTA tubes (Microvette®, SARSTEDT AG & Co., Germany) for determination of the white blood cell count (VetABC, Scil animal care company GmbH, Germany).

3.6.3 Micro computed tomography

Micro computed tomography scans (VivaCT40, Scanco Medical AG, Switzerland) of the rat skull were performed while immobilizing the animal in a custom-made holder (Figure 9) under Sevoflurane anesthesia as described in 3.4.1. The animals were scanned directly postoperatively, two weeks after surgery and after euthanasia (four

weeks after surgery). Under the laminar air flow hood (Phantom Animal Transfer Station, Allentown Inc, United States), the animals were placed in sternal recumbency and the holder was closed at its best to protect the animal from the scanners environment (Figure 10). The holder had a built-in heating system to avoid heat loss of the animal during the scanning which lasted approximately 30 min. The region of interest was scanned using 70 kVp, 114 µA, 200 ms integration time and a 38.9 mm field of view reconstructed across an image matrix size of 2048 x 2048, resulting in an isotropic voxel size of 19 µm. The acquired scan data of the three time points were registered to each other using IPL (Image Processing Language) provided by the manufacturer. Bone volume at each time point as well as bone evolution over time was evaluated within a cylindrical volume of interest (VOI; d=263 pixels) which was fitted into the defects created during surgery. The identical VOI was then applied to the later time points. Bone volume, present in the VOI after surgery, was subtracted from all time points.

Figure 9: Custom-made holder: showing the extension for the animal's head and its fixation in the anesthetic mask. **A**: without rat from above, **B**: with rat in place from above, **C**: with rat in place lateral

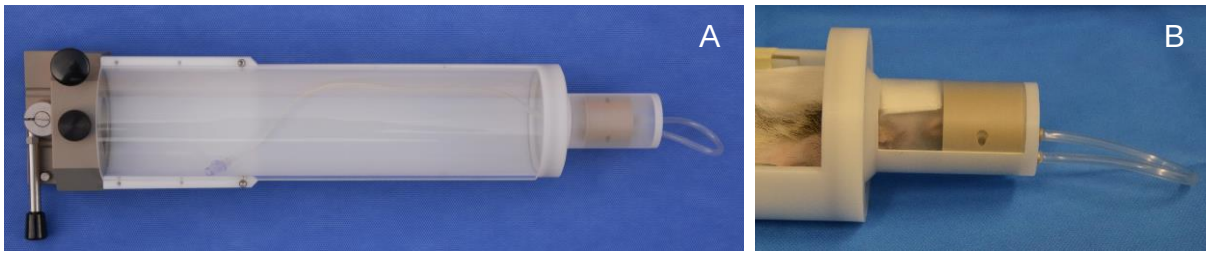

Figure 10: Closed custom-made holder: A: without rat (heating system not shown), **B:** with rat in place

3.6.4 Fluorochrome labeling

The fluorochrome Xylenol Orange was injected three weeks post-surgery (90 mg/kg BW, subcutaneously) to visualize bone formation and bone remodeling in histological sections. Xylenol Orange is incorporated in newly formed calcified tissues that allow showing which bone calcified at the time of administration of the dye.[27]

3.7 Euthanasia, sample harvest and post mortem evaluations

3.7.1 Euthanasia

After putting the animals in Sevoflurane anesthesia four weeks post operatively, the animals blood was withdrawn from the tail vein as described in 3.6.2 and samples were collected for PRIA-Testing as described in 3.2.3. Thereafter the animals were euthanized by intracardial puncture and administration of an overdose of Pentobarbital (200 mg/ml; 0.6 ml Esconarkon® (Streuli Pharma AG, Switzerland) mixed with 0.3 ml sodium solution (NaCl 0,9 %, B. Braun Melsungen AG, Germany). The animals were always separated from other animals before euthanasia and euthanasia was carried out in a separate room by a veterinarian.

For all animals euthanized, a macroscopic examination of the external body surface, all orifices and surgery sites was conducted. After euthanasia, animals were weighed and the head was scanned with CT.

3.7.2 Sample harvest

The calvaria without soft tissues with the two defects were cut from the skull using an oscillating saw. The right caudal corner was cut off to mark the bone fragment for orientation (Figure 11). Samples (Figure 12) were transferred in 70% Ethanol.

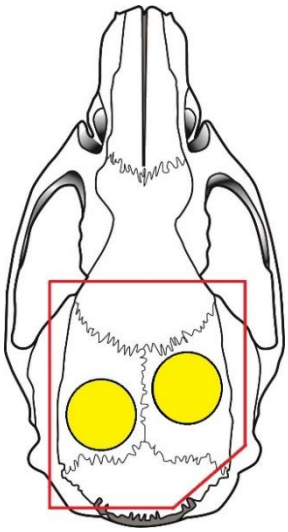

Figure 11: Position and marking of bone sample to be cut from skull after euthanasia.

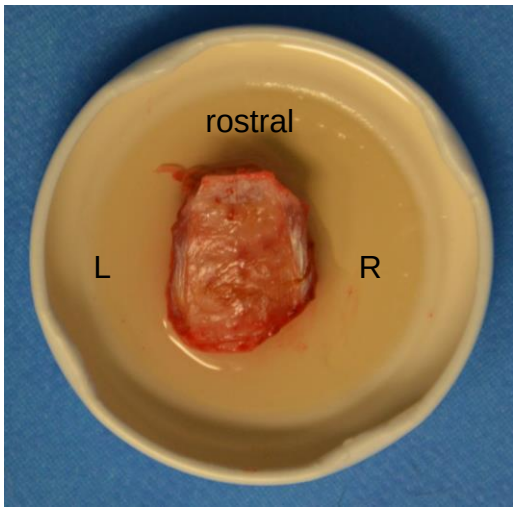

Figure 12: Harvested calvaria

3.7.3 Histology

3.7.3.1 Histological processing

The samples were fixed in 70% ethanol (Alcosuisse, Switzerland) for four weeks, with at least one change to fresh solution per week, before continuing with the processing. During the fixation time, contact radiographs of the samples were made using a Faxitron X-Ray Cabinet (#43855A, Faxitron X-Ray Corporation, Schweizer AG, Switzerland) applying a voltage of 20kV, no filter and an exposure time of 40 seconds, using a high-resolution film (D4 Structurix, AGFA, Belgium) and developed (AGFA Structurix NDT-M eco Developer, AGFA, Belgium). The samples were then dehydrated through an ascending series of ethanol (70%, 96%, and 100%; Alcosuisse, Switzerland) with two changes for each step, transferred to xylene (Brenntag Schweizerhall AG, #10934-550, Switzerland) for four days and then finally to methyl methacrylate (Sigma-Aldrich Chemie GmbH, #5590-9, Switzerland) for embedding. First the samples were put into MMA I solution for three days, afterwards into MMA II solution for three days and stored refrigerated (4°C). For additional five days, the samples were applied to MMA III solution with a softener, dibutyl-phthalate (Sigma-Aldrich Chemie GmbH, #524980, Switzerland) and also stored refrigerated

(4°C). To prevent overheating during polymerization the samples were further cooled in a water bath for seven days at room temperature. After the polymerization was completed they were hardened in an oven at 40 – 60°C overnight.

The polymerized samples (Figure 13) were trimmed using a butcher saw so that they could be glued (cyanoacrylate adhesive, Cyanolit, Panacol-Elosol GmbH, Germany) onto holders to fit into annular blade saws (Leica SP 1600 saw microtome, Leica AG, Biosystems AG, Switzerland) and sectioned. Serial sections, cut in a coronal plane, of around 500 µm were made around the center of each sample.

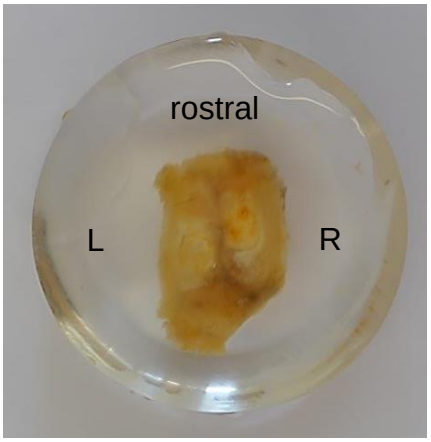

Figure 13: Fixed sample embedded in MMA (ready for cutting)

Before proceeding any further, contact radiographs were made, this time not of the full thickness samples but of the sections. Two sections of each defect side, which were the most central in the defect, were chosen for further processing (Figure 14).

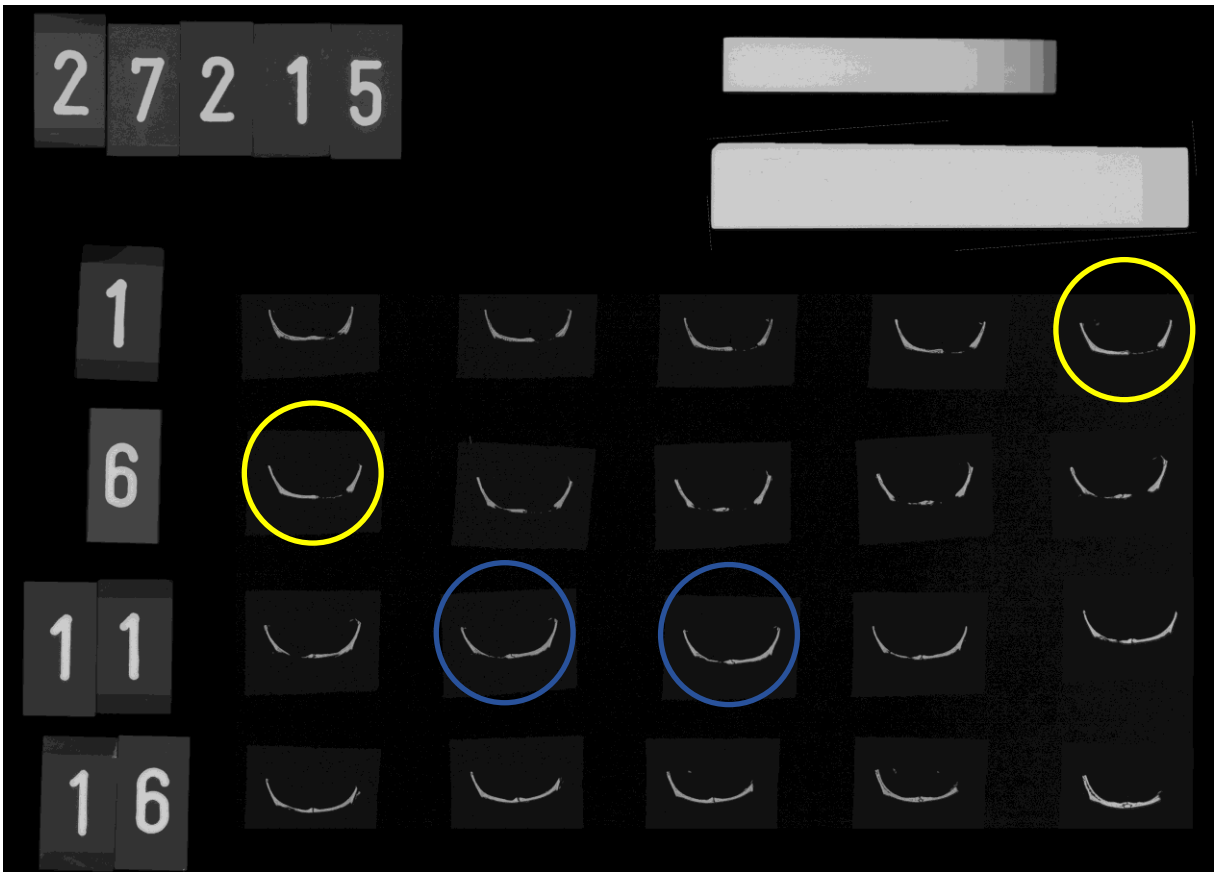

Figure 14: Contact radiograph of the un-glued, not-ground thick-sections displaying the process of choosing the sections for further proceeding. In this case sections # 5 and 6 (yellow circles) were chosen for the right defect, sections # 12 and 13 for the left defect (blue circles). (The number in the upper left corner gives the resin-block # [here 27215 corresponds to animal # 1]. The numbers at the left side give the number of the individual slide [here 1, 6, 11, 16 up to a total of n= 20]).

The sections were glued onto opaque Plexiglas slides (75x25x2mm, Semadeni AG, Switzerland), ground and polished (Exakt Micro Grinding System, Exakt Apparatebau, Germany), using varying roughnesses of grinding papers (P1200, P2400 and P4000, Struers GmbH, Switzerland), to obtain a final thickness of around 125 µm.

One of the sections of each defect side remained unstained for the observation of the fluorochrome labels. For the staining, the sections were etched using 1% formic acid (Fluka #06460, Sigma-Aldrich, Switzerland) for 30 seconds. Then the slides were rinsed with tap water for five minutes before they were stained with a 15% Giemsa solution (Fluka Analytical #48900, Sigma-Aldrich, Switzerland) heated to 55°C for 45 minutes, rinsed for 5 minutes and counterstained with a 1% Eosin working solution

for 2 minutes, containing 1% Eosin stock solution (Eosin Yellowish, Fluka #45240, Sigma-Aldrich, Switzerland) and acetic acid (Glacial Acetic Acid, Fluka #45731, Sigma-Aldrich, Switzerland). Finally, the slides were differentiated for two seconds with 70% ethanol, then five seconds in 96% ethanol and dehydrated two times with absolute ethanol for two minutes each.

3.7.3.2 Microscopic Evaluation

The microscopic evaluation was performed blinded by a veterinarian pathologist (FTA Pathology and Toxicopathology, Germany) and by the author using a discussion microscope (U-DO3, Olympus Corporation, Japan). With the use of the GE-stained slides, the defect healing was semi-quantitatively analyzed applying a grading scheme (grade 1= minimal, grade 2= slight, grade 3= moderate, grade 4= marked, grade 5= massive, Table 4). Special attention was given to regenerative and reparative tissue changes, including newly formed calvarial bone (relative amounts/percentage of defect closure, thickness, vascularization, necrosis), changes at the soft tissue (e.g. fibrous/fat/muscle tissue), and at the collagen membrane (remnants, degeneration) in the defect. Furthermore, other changes like hemorrhage, hemosiderin deposition, inflammation (lymphocytic/granulocytic/granulomatous), metal remnants or damage of adjacent tissue structures were analyzed, as well as the defect closure over the length of the defect with newly formed bone in %. A defect closure of estimated 1-20 % corresponded to a grade 1, up to 40 % to a grade 2, up to 60 % to a grade 3, up to 80 % to a grade 4 and a defect closure of estimated up to 100 % to a grade 5.

The metal remnants were only graded with P=present or 0=not present.

Table 4: Histological grading

Grade	Grading general	Grading defect closure
1	minimal	1-20 %
2	slight	-40 %
3	moderate	-60 %
4	marked	-80 %
5	massive	-100%

3.7.3.3 Epifluoroscopic analysis

To compare bone formation over time, a semi-quantitative analysis of fluorochrome (Xylenol Orange) labelled mineralization lines was performed blinded on unstained thick sections using a fluorescence microscope (AxioPlan2 Microscope, Zeiss, Oberkochen, Germany) applying a grading scheme (grade 1= minimal, grade 2= slight, grade 3= moderate, grade 4= marked, grade 5= massive).

3.8 Statistical evaluation

The data was checked for normal distribution by exploring qq-plots as well as using the Shapiro-Wilk normality test. Since the data was not normally distributed, a non-parametric ANOVA in order to determine the influence of the treatment (organized into groups A, B, C) was used thereafter. Such an analysis was performed for the CT bone volume at both times (2 and 4 weeks), the inferred bone growth as well as for the histological data (Defect Closure, Thickness, Vascularization). The bone growth was calculated as the change in bone volume normalized by the time between the two measurements. In addition, another non-parametric ANOVA was performed in order to determine whether or not the white blood cell (WBC) decreased over time. The associated test for all non-parametric ANOVA's was the Kruskal-Wallis Rank sum test, and the significance level was fixed at 0.05. The analysis was done using the R project for statistical computing (https://www.r-project.org).

4 Results

4.1 Inclusion criteria, excluded animals and group size

All twelve animals enrolled into the study fulfilled the inclusion criteria at the beginning of the study as described in 3.2.1 with an age of minimum 13 weeks (eight animals) and a maximum of 17 weeks (one animal). This results in a mean age of 13.4 weeks with a standard deviation of 1.3.

All rats were considered healthy based on their health certificate (Charles River EEW29863) and the preanesthetic clinical examination. In total three out of the twelve rats had to be excluded. The animal numbers and reasons for exclusion are summarized in Table 5.

Animal # 0 was replaced immediately, since the membranes with the cells were not yet placed in the animal as it passed away. Animal # 10 died in anesthesia during CT when the membranes with cells were already located in the animal. Because no additional sorted cells were available, we could only replace the defect with group C. The other defect in this animal was left empty. Animal # 2 in which there was a brain injury during surgery could not be replaced because no more animals were available.

Table 5: Exclusions

Animal #	Group Left/right defect	Reason for exclusion	Replacement
0	NA / NA	died before surgery during anesthesia - stopped breathing	Both groups (animal # 1)
2	C / B	surgery: brain injury and prolapse – euthanasia	No
10	C / A	died during CT anesthesia post-OP - stopped breathing	Only group C (animal # 11)

Therefore, a total of nine animals were included in the analysis (Table 6). Thus, six defects each in groups A and B and five defects in group C were included (Table 7).

Table 6: Animals included in analysis

Animal #	Left defect filled with group	Right defect filled with group
1	B	C
3	C	B
4	A	B
5	A	C
6	B	A
7	C	A
8	A	B
9	B	A
11	C	Empty

Table 7: Number of defects per group included in analysis

Group	Description	Number of defects included in analysis
A	Cells sorted on their Runx2/Sox9 ratio seeded on collagen membrane	6
B	Unsorted cells seeded on collagen membrane	6
C	Collagen membrane only	5

4.2 Injuries to the dura mater intraoperatively

Out of the 22 drilled defects the dura mater was injured in four defects although using the drilling technic as described in 3.4.2 Surgical procedure. As shown in Table 8 a small hole up to 1 Millimeter was generated in the dura mater within three defects (one in group B, two in group C). In animal # 2, the dura and brain were damaged because of a too deep drilling. This animal was euthanized and excluded. In two defects, we could observe a subdural hematoma without a dura mater injury.

Table 8: Dura mater injuries intraoperatively

	left dura mater intact			right dura mater intact		
Animal # (group left/right)	yes	no	comment	yes	no	comment
1 (B/C)	x				x	small hole, approx. 1mm
2 (C/B)	x				x	brain injury and prolapse
3 (C/B)	x			x		
4 (A/B)	x			x		
5 (A/C)	x			x		
6 (B/A)	x			x		
7 (C/A)	x			x		hematoma subdural
8 (A/B)	x				x	small hole, no prolapse
9 (B/A)	x			x		hematoma subdural
10 (C/A)	x			x		
11 (C/emp.)		x	small hole <1mm	x		

4.3 Health monitoring

The results of the rat Surveillance PRIA (PCR Rodent Infectious Agent) analyzed by Charles River Research Animal Diagnostic Services, USA were all negative two weeks before surgery and at the time of euthanasia.

4.4 Weights

The animals included in the study had a weight of 200 g ± 20 g. Seven out of nine animals lost weight after the surgery. The maximum weight loss was 9% (mean of 2% with a standard deviation of 3.2) in the first week and up to 7% (mean of 2%, standard deviation 2.5) in the second week compared with the body weight at surgery. All animals reached their pre-OP weight or even gained weight after three weeks after surgery. From this time on all animals could keep their post op weight or even weighed more than before the surgery (Figure 15).

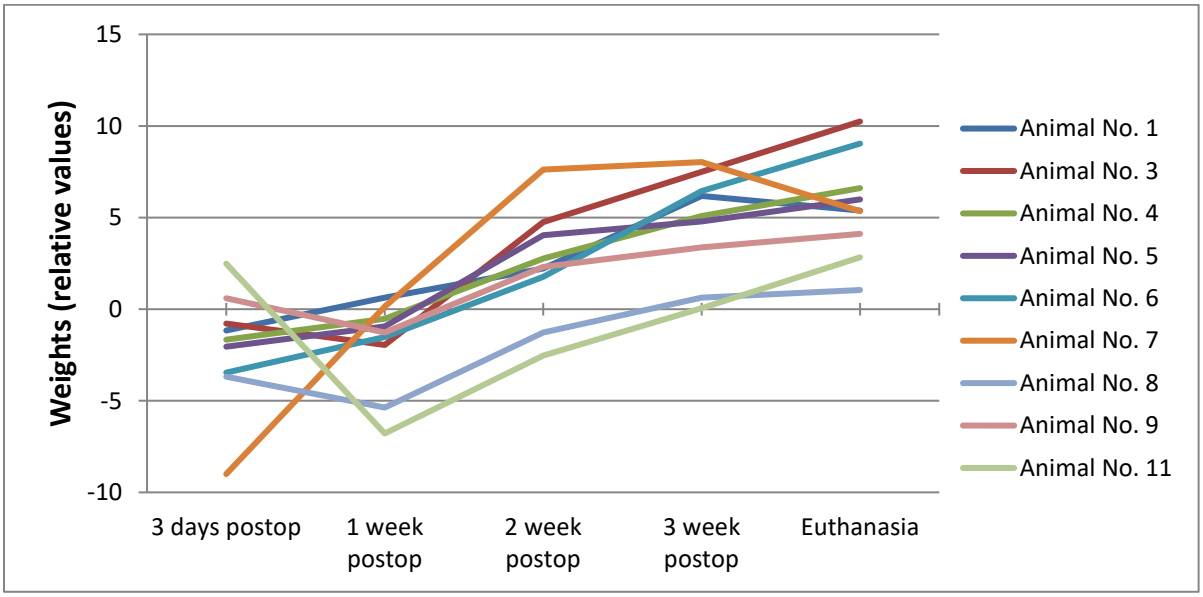

Figure 15: Change in body weights in % compared to the preoperative weight

4.5 White blood cell count

The white blood cell count, as a systemic measure able to indicate acute inflammation, was determined for each animal at time of surgery, after two weeks and at time of euthanasia (Figure 16). The values measured were mostly beneath the

physiological healthy range (2-7 Tsd. leukocytes/µl) for RNU nude rats as described by Bani Ismail *et al.* [28]. The WBC levels significantly decreased over time (chi=5.85, p=0.05).

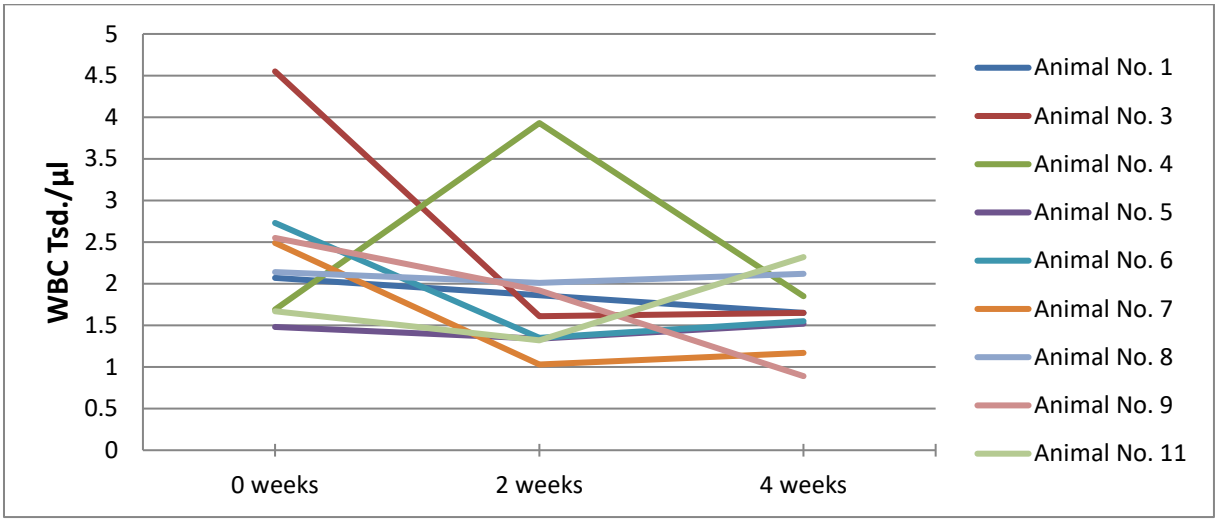

Figure 16: White blood cell count (Tsd./µl)

4.6 Animal welfare

The following scores were documented: During the first three days after surgery a score of zero to three was observed in the animals, with a score of three being observed only in two animals on the evening of the surgery due to huddled/inactive (two points) and partial head tilt (one point). By day six the value for the score was between zero and one. From week three on all animals had a score of zero. The highest score which we could observe across all groups at all time points was three.

4.7 Necropsy

During necropsy abnormalities were found in two rats. In animal # 7 the left defect was higher and the right defect was deeper and darker than the surrounding tissue. Animal # 9 showed red spots on both defects (Figure 18).

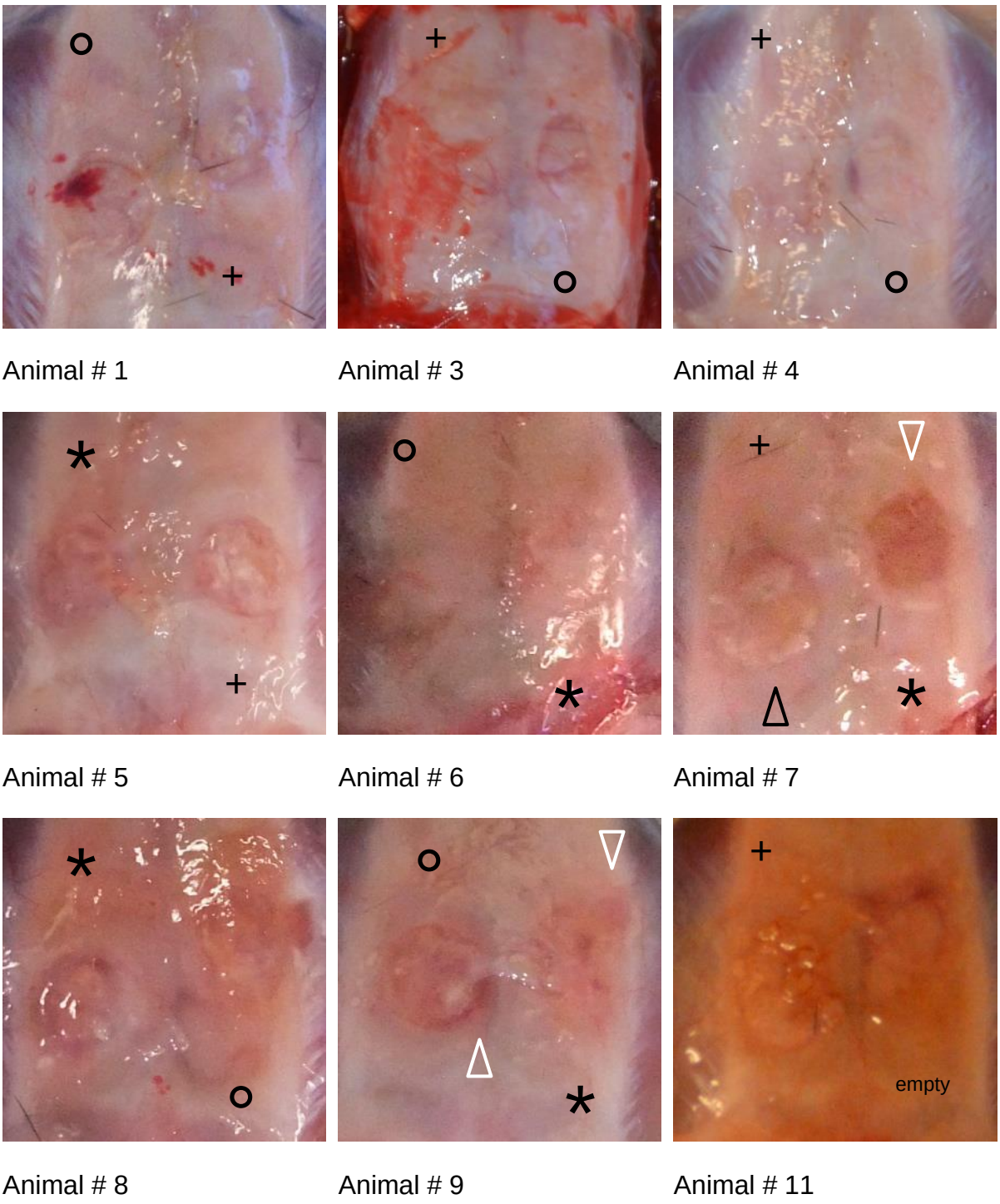

Figure 17: Overview calvaria after dissection, orientation: top always rostral, left always left; Note in animal # 7 the left defect was higher (open black arrow head) and the right defect was deeper and darker than the surrounding tissue (open white arrow head). Animal # 9 showed red spots on both defects (open white arrow heads). * = group A, ° = group B, + = group C

4.8 Micro computed tomography analysis

To monitor the healing process and new bone formation over time, CT scans were performed at two and four weeks post op (euthanasia) as indicated in 3.6.3. Healing was assessed by comparison of these scans with images taken directly post-operatively. A representative 3D reconstruction of microCT images is given in Figure 18 (for an overview of all individual defects see Attachments). Only the bone of the cranium is shown in the images. New bone formation in between time points is highlighted in orange.

A

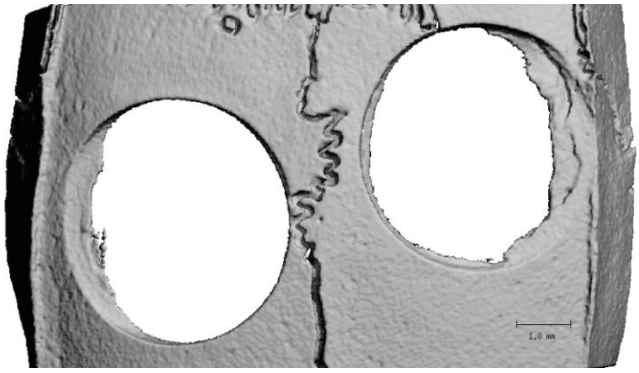

B

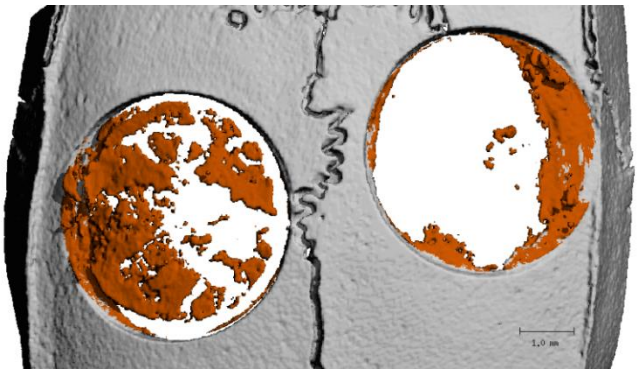

C

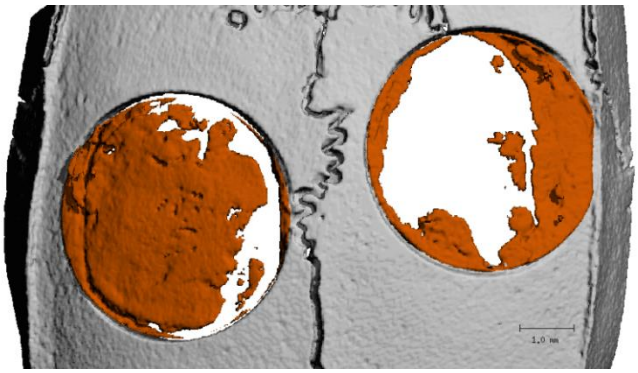

Figure 18: Representative 3D reconstruction of the cranium, animal # 3: A: post op, **B:** after two weeks, **C:** after four weeks**.** New bone formation in between time points is highlighted in orange. Rostral: always shown at top of the picture.

None of the animals could heal the defect in the observation period. Defects of group A and B showed similar healing outcomes after two (mean 0.486 and 0.488 mm^3; SD=0.197 and 0.192) as well as after four weeks (mean 1.798 and 1.860 mm^3; SD=0.693 and 0.611) based on the bone volume. Group C showed an increased bone volume in the defect compared to group A and B both after two (mean 0.810 mm^3; SD=0.458) and four weeks (mean 2.362 mm^3; SD=1.043). Nevertheless, the CT data revealed no significant influence of the group (=treatment) factor (bone volume after two weeks: chi=1.12, p=0.57; bone volume after four weeks: chi=1.35, p=0.51; inferred bone growth: chi=1.06, p=0.59). However, the bone volume measured with CT significantly increased over time (chi=21.144, $p<0.05$).

The three defects with an injury of the dura mater (Table 8) showed a decreased healing after two weeks post OP compared to the other defects of their group. After four weeks this decreased healing was still present in two defects (animal # 1 right defect, # 8 right defect). The left defect of animal # 11 has caught up between two and four weeks.

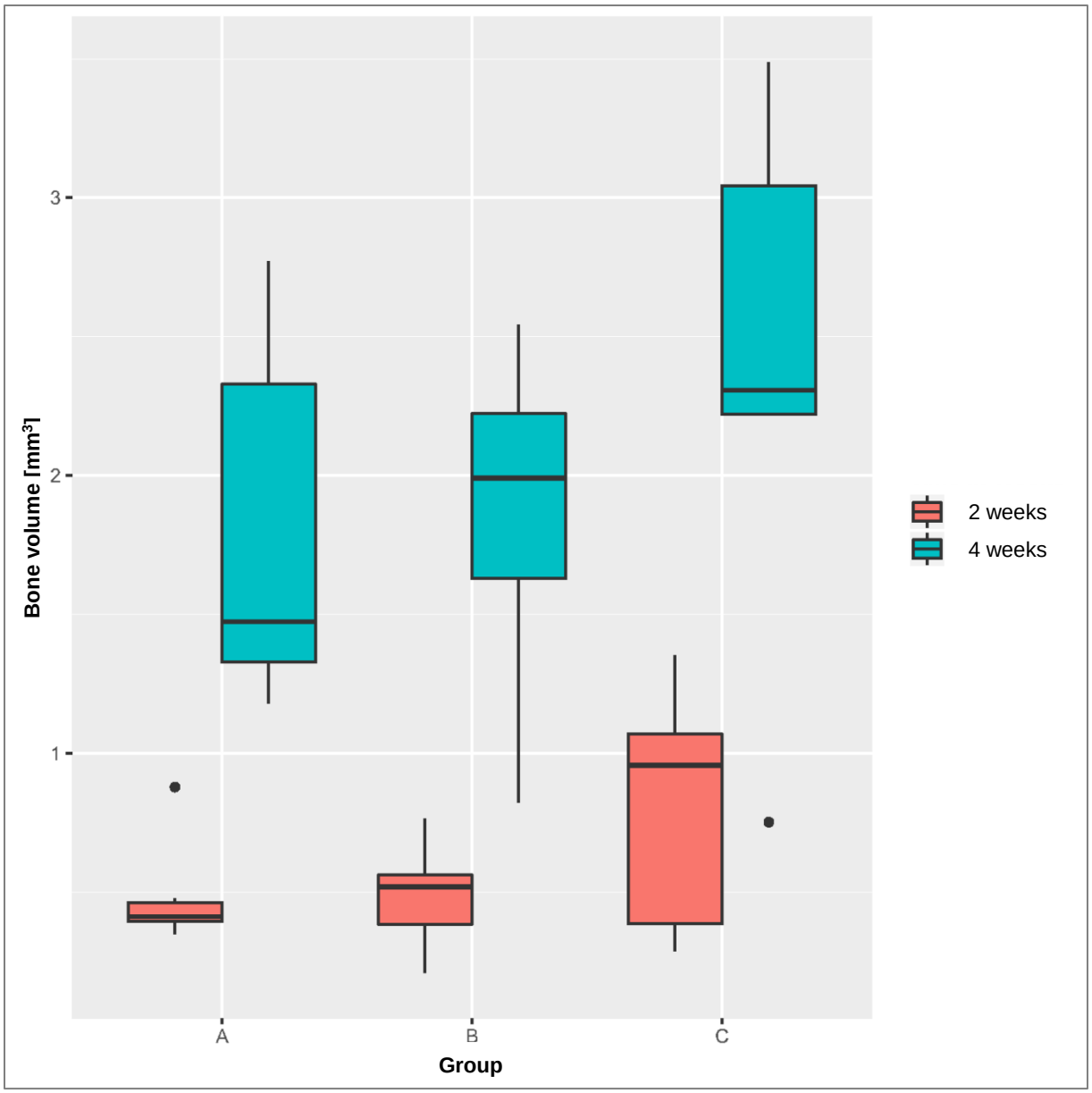

Figure 19: Bone volume per group at two and four weeks

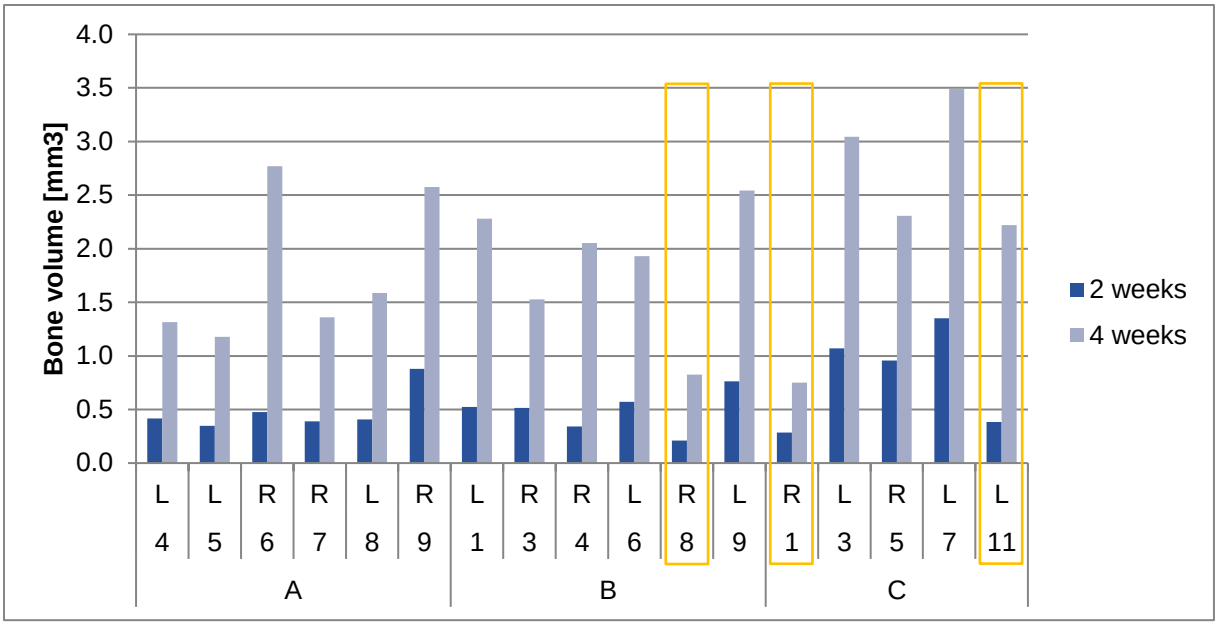

Figure 20: Bone volume per defect. Defects with dura mater injury are orange bordered. L (left) and R (right) marks defect side, # = animal #

Additionally to the three groups, one defect of animal # 11 (right side) was left empty (no membrane and no cells). This defect had formed less new bone after two and four weeks than all defects of group A, B and C. After two weeks it had a new formed bone volume of 0.172 mm^3 compared to 0.348 mm^3 (group A), 0.210 mm^3 (group B) and 0.286 mm^3 (group C) as the lowest values in these groups. The same ratio was observed after four weeks: the empty defect had formed 0.656 mm^3 new bone compared to 1.179 mm^3 (group A), 0.824 mm^3 (group B) and 0.752 mm^3 (group C) as the lowest values in these groups. However, for these values, it must be mentioned that the lowest values of groups B and C belong to defects with an injury of the dura mater. The values of the defects without dura mater injury are higher as shown in Figure 20.

4.9 Histology

Generally, the mean defect closure by formation of new calvarial bone after four weeks was of moderate to high grade. So, defects treated with membrane only had the highest defect closure (group C: mean grade 4.0) compared to defects treated with membrane + unsorted hBMSC (group B: mean grade 3.2), membrane + sorted hBMSC (group A: mean grade 3.2), and empty defect (grade 1.0). However,

individual values in each group (intra-group variation) ranged from grade 1 at the lower end, up to grade 5 at the higher end and therefore exhibited a pronounced standard deviation (membrane only [group C]: SD= 1,6; membrane + unsorted hBMSC [group B]: SD= 1.5, membrane + sorted hBMSC [group A]: SD: 1.5).

Table 9: Defect closure, *: grade 1: 0-20%, grade 2: 21-40%, grade 3: 41-60%, grade 4: 61-80%, grade 5: 81-100%

Defect closure	Group A (n= 6)	Group B (n= 6)	Group C (n= 5)
mean defect closure by new bone, [graded 1-5] *	3.2	3.2	4.6
standard deviation [SD]	1.5	1.5	1.6

Microphotographs of the defects of group A are shown in Figure 21, of group B in Figure 22 and of group C in Figure 23.

No cartilage tissue could be found in any defect of any group.

Thickness of the new calvarial bone was relatively low and generally not reaching the original levels (mean grades: 2.0 – 2.4) with the lowest mean grade in group A (2.0) and the highest mean grade in group C (2.4). All grades between 1 and 3 were found in each group. No defect had reached a thickness of a grade 4 or 5.

Vascularization was low to moderate (mean grade 1.8 – 2.4). The highest mean grade was again observed in group C (2.4) whereas the lowest mean grade was found in group B (1.8). The highest grade overall groups was 4 and only found in one animal (animal # 6, right defect, group A; Figure 21). All other defects were between a grade of 0 and 3 with all grades found in each group. An example of new formed blood vessels is shown in Figure 24.

Osteonecrosis, characterized by small areas of empty osteocytic lacunae, was of low severity and occurring at low incidence (group A: mean severity 0.5 [incidence 2/6]; group B: mean severity 0.2 [incidence 1/6]; group C: mean severity 1.0 [incidence 3/5])

Severity of granulomatous inflammation in the soft tissue was low and occurred around exogenous material (membrane and suture material) as well as endogenous material (hairs) with a mean grade of 0.8 – 1.2 and an incidence of 5/6 (group A and B) respectively 4/5 (group C).

Light pink coloured acellular material (interpreted as membrane remnants) was visible in seven out of 17 defects with a membrane with an incidence of 2/6 (group A and B) or 3/5 (group C) per group. An example of the acellular material is shown in Figure 25. All defects with membrane remnants had a grade of 3 for the thickness of the new calvarial bone. This grade was only found in one additional defect out of the ten defects without light pink coloured acellular material. All other defects had a grade of 1 or 2 for the thickness of the new calvarial bone. In addition, all the defects with membrane residues had a high grade for vascularization (grade 2 to 4, mean grade 3).

Fluorochrome analysis of Xylenol Orange using epifluorescence microscopy showed red-orange marked lines not only in the periphery but also in the center of the defect (Figure 26). In the periphery, red-orange marked lines (Figure 27) were found in all defects of all groups with a grade between 1 and 2. In the center they were only found with an incidence of 3/6 (group A), 5/6 (group B) and 4/5 (group C).

Additionally to the defect area, there is also limited new bone formation at the endosteal area of the calvaria and around the vessels of the cortex (Figure 27).

In none of these histological parameters statistical significance was found.

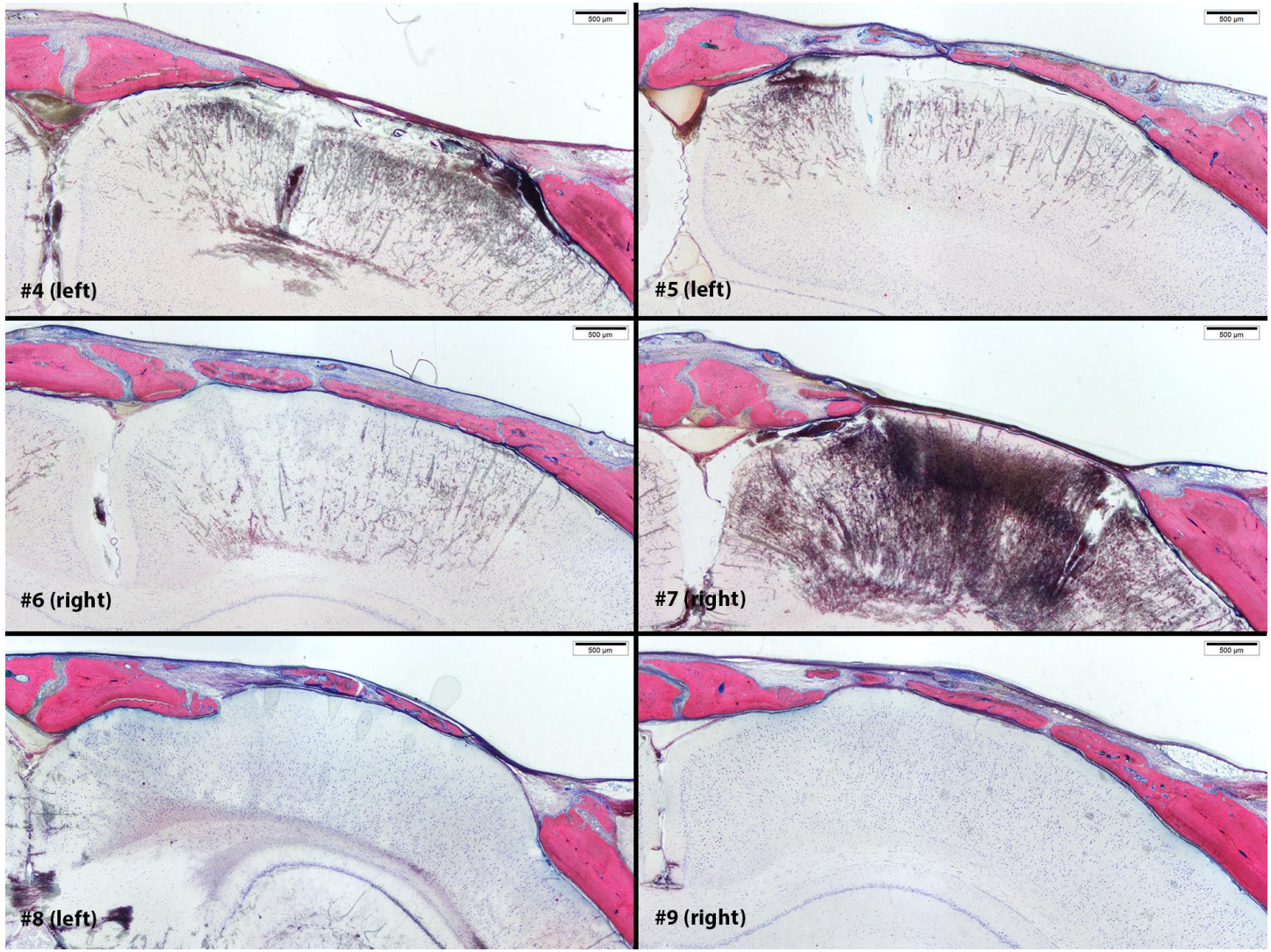

Figure 21: Microphotographs of calvarial defects of group A treated with collagen membrane and sorted cells (GE-stained, MMA-embedded thick-sections of the coronary plane through the defect center)

Note the inter-individual variation in defect closure ranging from very low (animal 7 [right]) up to nearly complete (animal #9 [right]). Newly formed bone does not the reach the thickness of the preoperative state (for easier comparison of the defects the midline is always shown at left side of the picture, images of right-sided defect are mirrored, # = animal #, bar 500 µm)

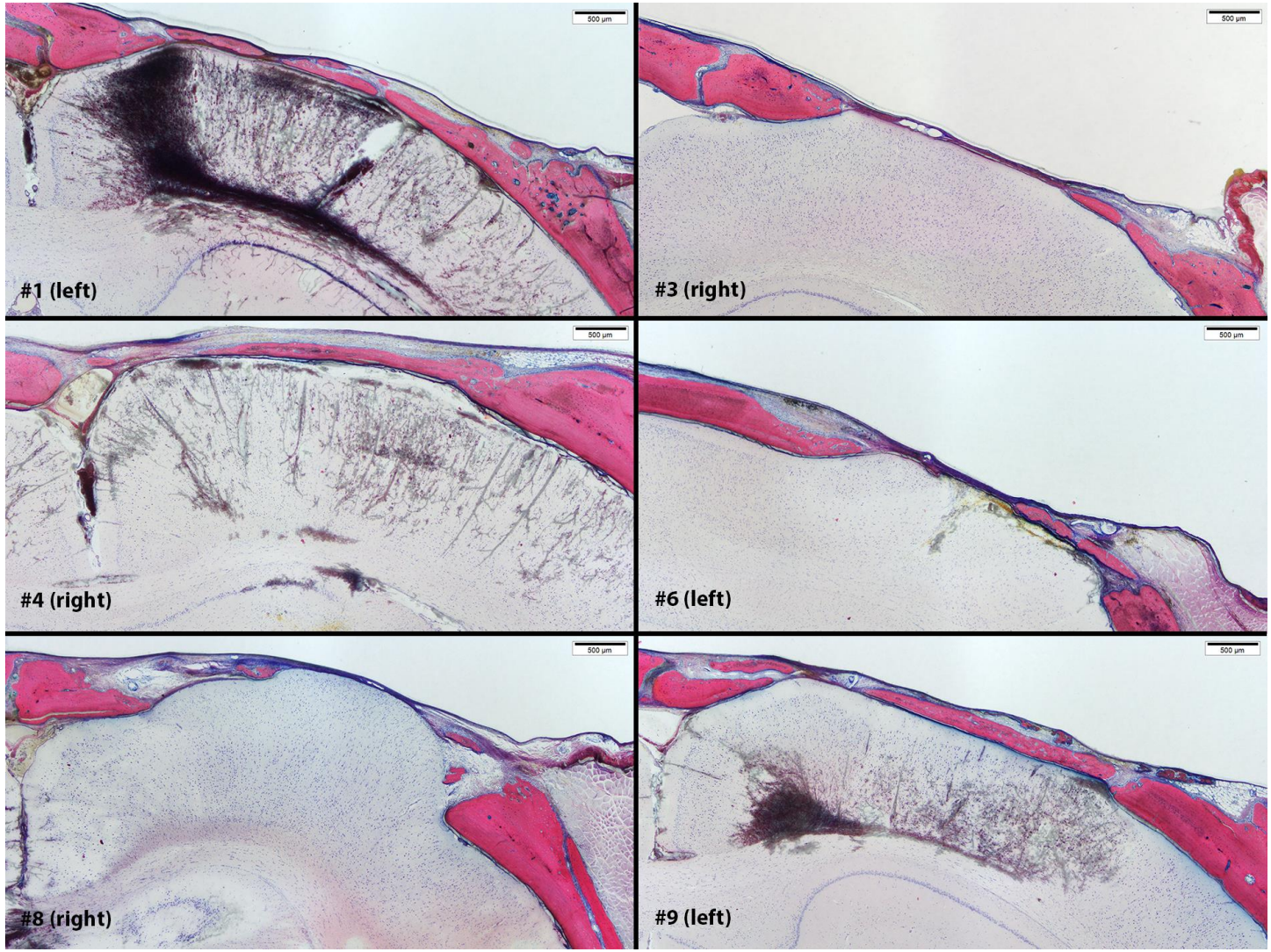

Figure 22: Microphotographs of calvarial defects of group B treated with unsorted cells on a collagen membrane (GE- stained, MMA-embedded thick-sections of the coronary plane through the defect center).

Note the inter-individual variation in defect closure ranging from very low (animal # 3 [right]) up to nearly complete (animal #1 [left]). Additionally, the newly formed bone does not the reach the thickness of the preoperative state. (for easier comparison of the defects the midline is always shown at left side of the picture, images of right-sided defect are mirrored, # = animal #, bar 500 µm)

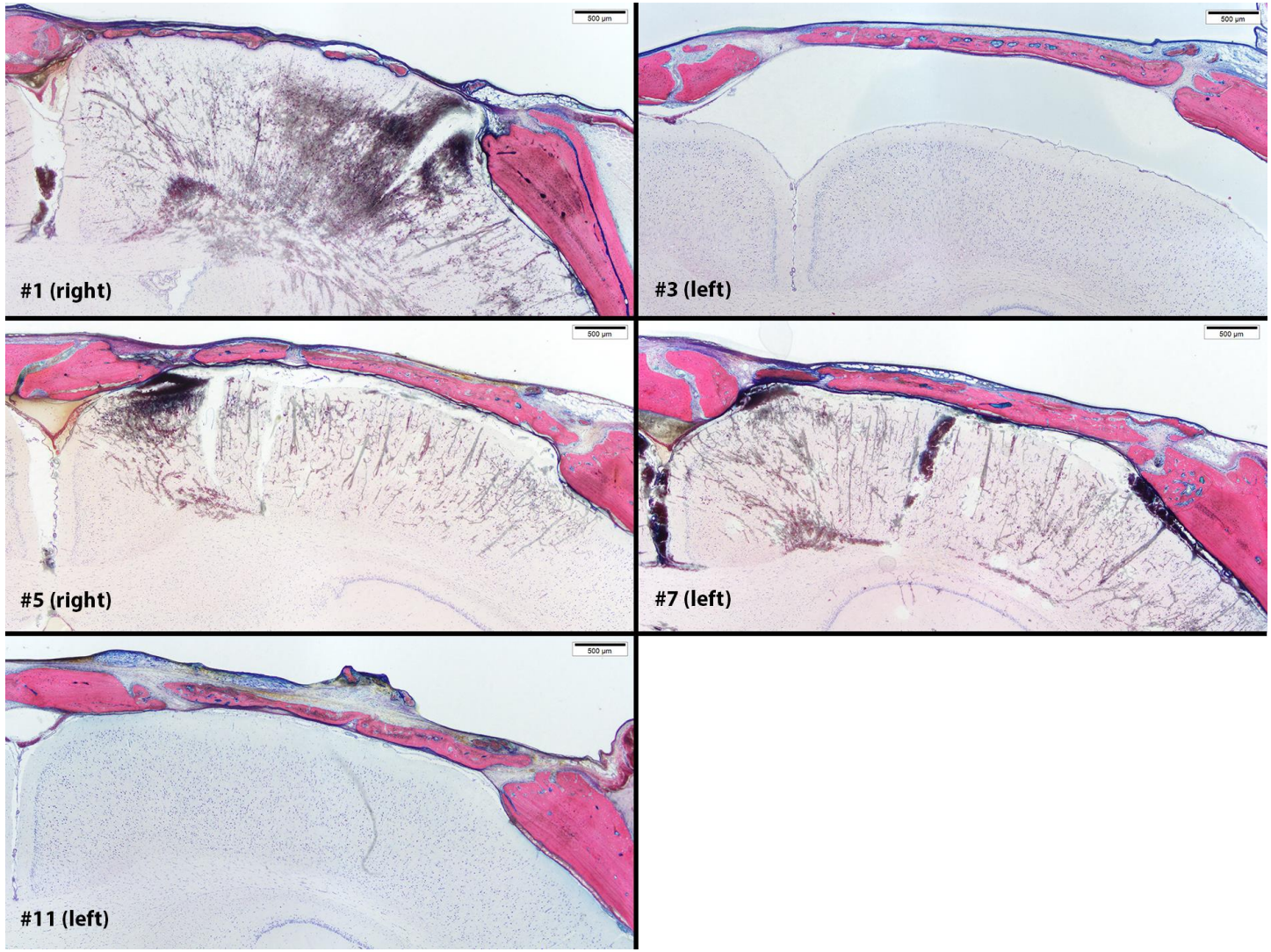

Figure 23: Microphotographs of calvarial defects of group C treated with collagen membrane, only (GE- stained, MMA-embedded thick-sections of the coronary plane through the defect center).

Note the inter-individual variation in defect closure varies less in this group from moderate (animal # 1 [right]) up to nearly complete (animal #1 [left]). The inter-individual variation of the thickness of newly formed bone varies from very low (animal # 1 [right]) up to moderate (animal #7 [left]). However newly formed bone does not the reach the thickness of the preoperative state. (for easier comparison of the defects the midline is always shown at left side of the picture, images of right-sided defect are mirrored, # = animal #, bar 500 µm)

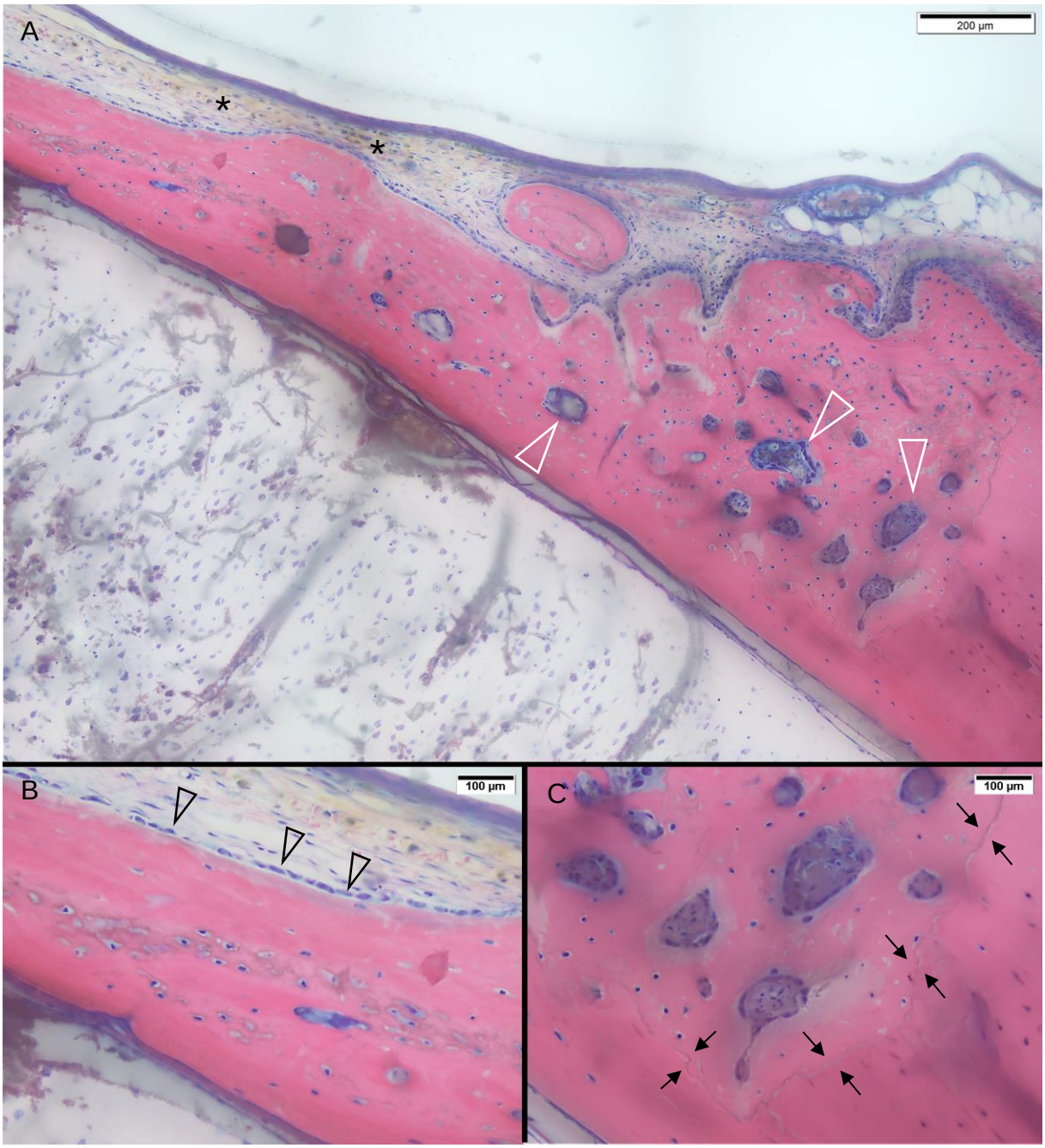

Figure 24: Microphotographs showing morphological features of the new bone formation (GE-stained slide of the left defect of animal # 1 [group B]). Note the general absence of cartilage tissue which characterizes the intra-membranous osteogenesis typical for calvarial bone. **A:** Overview (20x) shows the lateral aspect of the calvarial defect. The surgical cutting line is clear visible as is the difference in calvarial thickness (compare new bone [left] versus pre-existing bone [right]. Blood vessels are more frequent in the newly formed bone compared to the pre-existing calvarial bone (open white arrow heads) and hemosiderin (asterisks) in soft tissue above the newly formed bone, bar 200 µm. **B:** Detail (40x) of the newly formed bone with osteoblasts lining on it (open black arrow heads), bar 100 µm. **C:** Detail (40x) of the border between newly formed and existing bone (arrows: cutting line). The differences in the shade of the bone's pink staining is caused by the degree of calcification (lower calcification causes a lighter pink staining of younger bone), bar 100 µm.

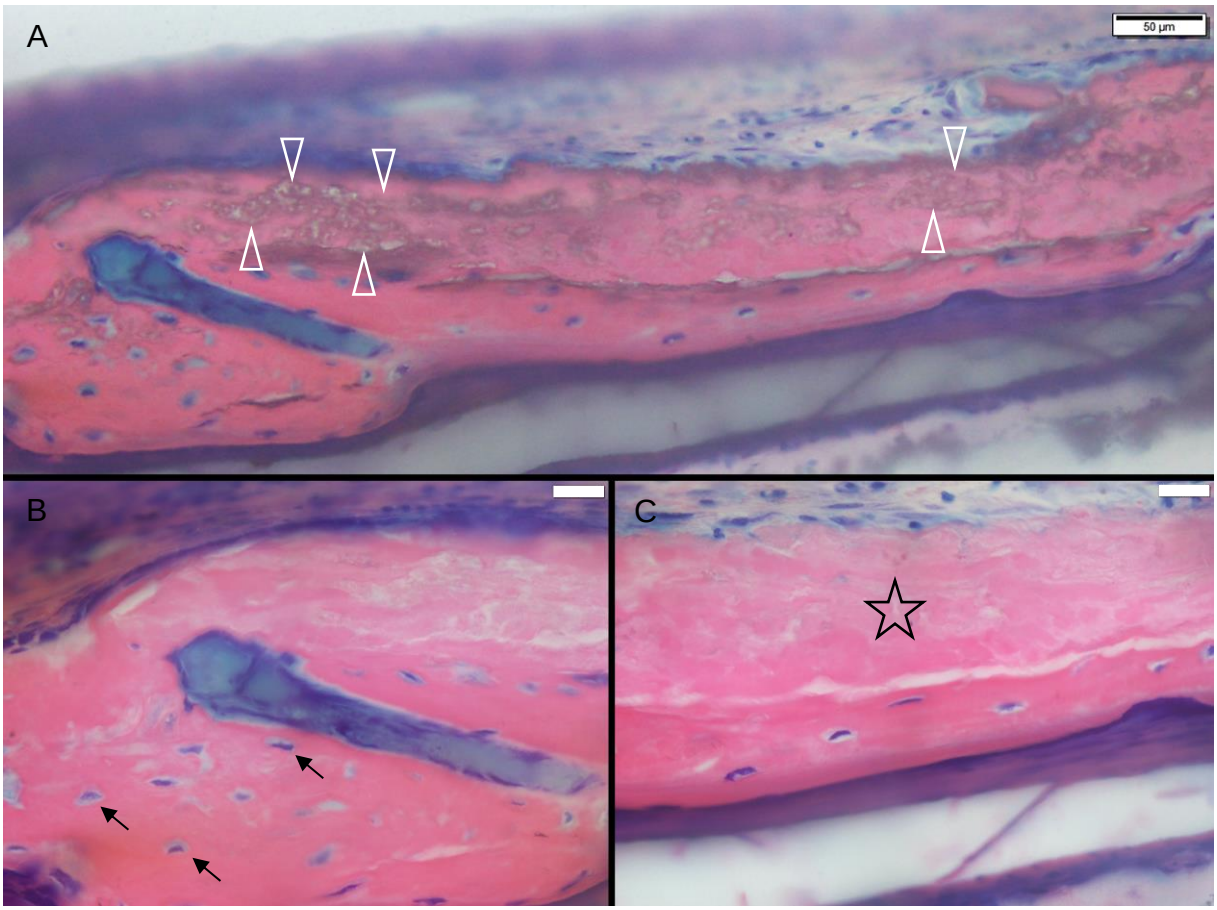

Figure 25: Microphotograph of the central defect area (GE-stained slide of the right defect of animal # 5 [group C]). **A:** Overview (40x) showing the difference between newly formed bone and the degraded collagen membrane (open white arrow heads), bar 50 µm **B:** Detail (100x, oil) of darker pink stained newly formed bone with cells (black arrows), bar 20 µm **C:** Detail (100x, oil) of light pink, acellular material (open black asterisk) interpreted as membrane remnants, bar 20 µm.

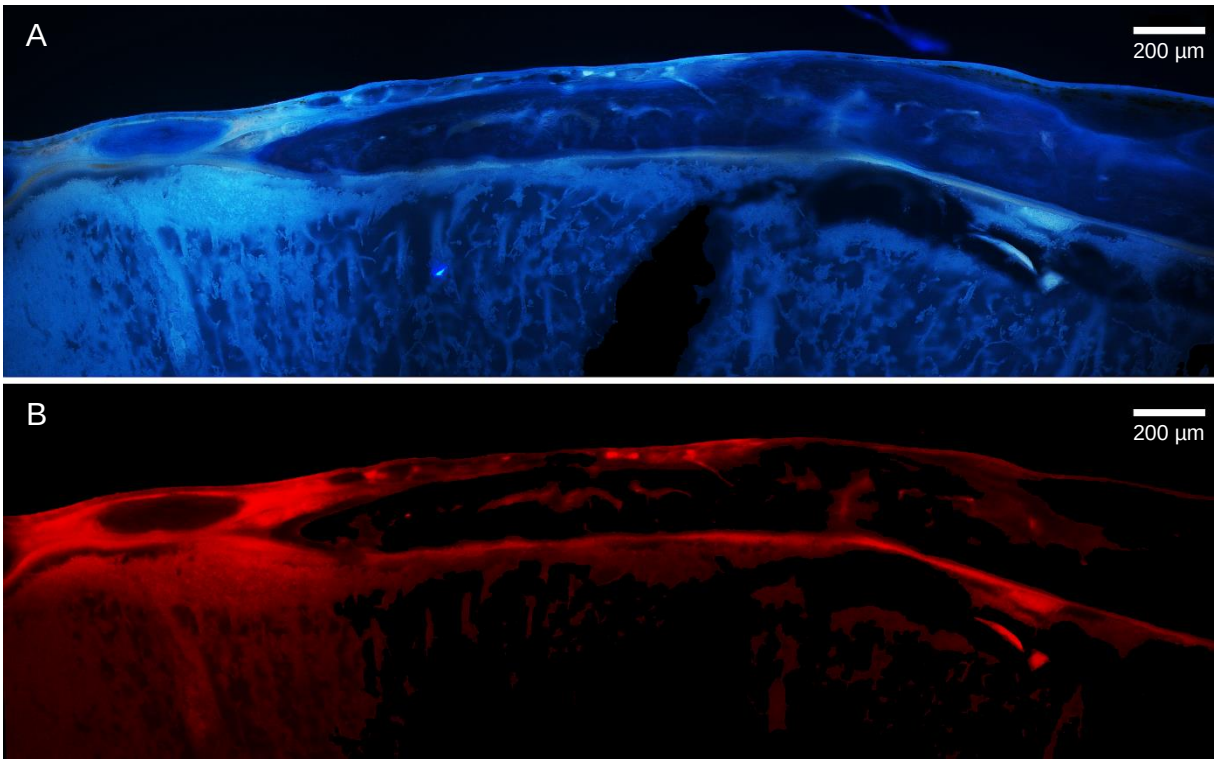

Figure 26: Overview-Microphotographs of the calvarial defect under epifluorescence (unstained slide, Xylenol Orange application at three weeks) animal # 1, left defect [group B]). **A:** Blue fluorescence caused by auto-fluorescence of bone and connective tissue. **B:** The red fluorescence is caused by incorporation of XO and shows the bone formation (and remodeling) at the time point three weeks post OP (the brown color of hemosiderin is an intrinsic property and not a result of staining). Bar 200 µm.

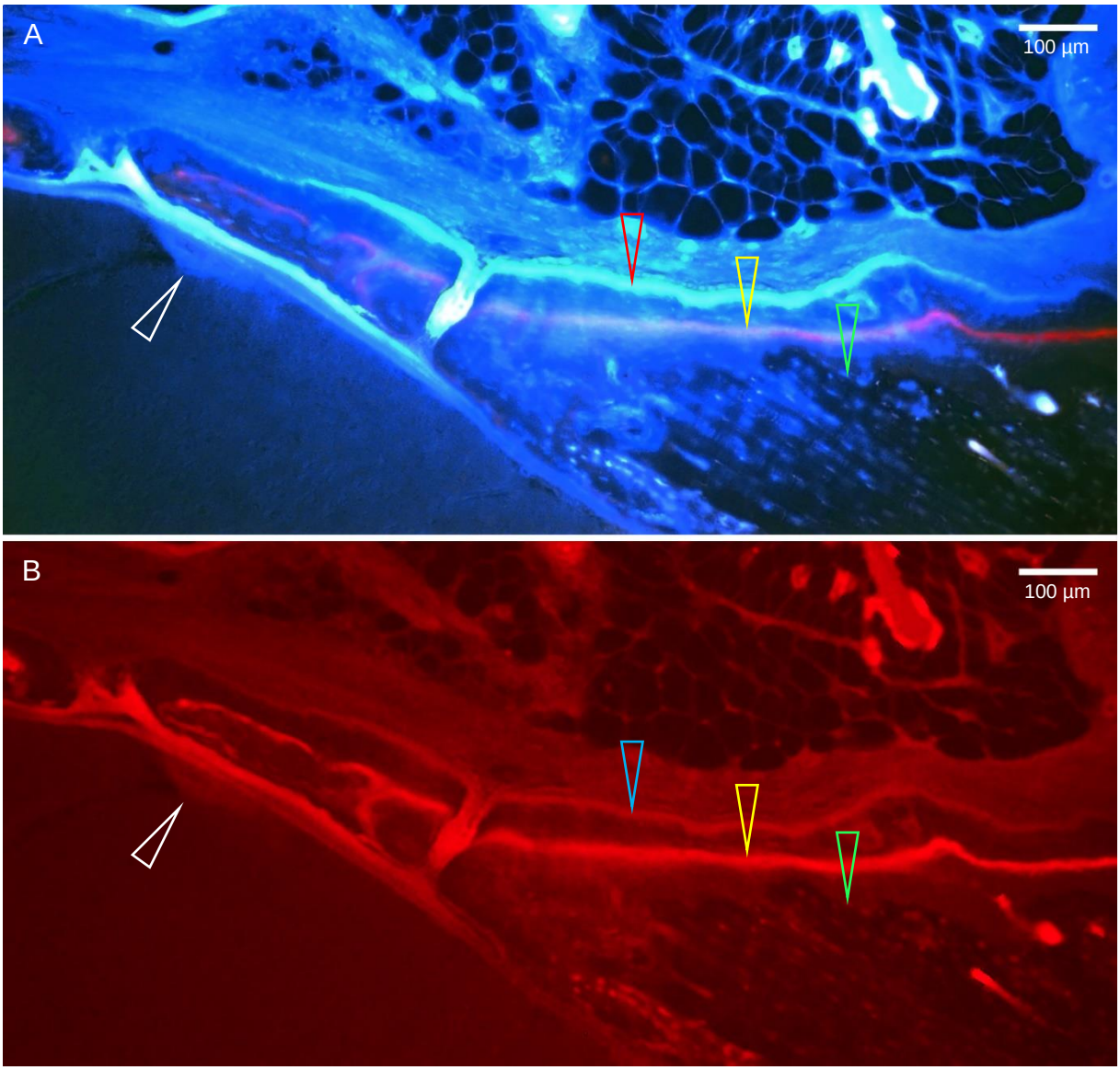

Figure 27: Microphotographs of the new bone formation at the lateral edge of the calvarial defect investigated under epifluorescence (unstained slide, XO application at three weeks, sample of animal # 3, left defect [group C]). **A and B:** Note the bright red line in the newly formed bone area (yellow arrow head) formed in continuity onto the pre-existing calvarial bone (green arrow head) without cartilaginous precursor tissue (intra-membranous osteogenesis). This line is caused by binding of the bone-seeking dye (XO) on Ca-ions in the matrix during new bone formation at timepoint three weeks post OP. Be aware, that even after timepoint three weeks post OP the bone formation is still ongoing (red arrow head in A / blue arrow head in B marks the bone at necropsy: four weeks post OP). Additionally to the defect area, there is also limited new bone formation at the endosteal area of the calvaria (white arrow head; growth related thickening), and around the vessels of the cortex (remodeling). Bar 100 µm

Additionally to the three groups, one defect of animal # 11 (right side) was left empty (no membrane and no cells). In the histological analysis this defect showed a very low defect closure (grade 1). Only directly at the edge of the drill hole some new bone was formed, but not in the center of the defect. No vascularization could be found in this small amount of new formed bone, as well as no necrosis. Slight granulomatous inflammation was observed especially around suture material remnants.

Since no new bone was formed in the center of the defect, a red-orange fluorescence signal could be observed only in the periphery and not in the center.

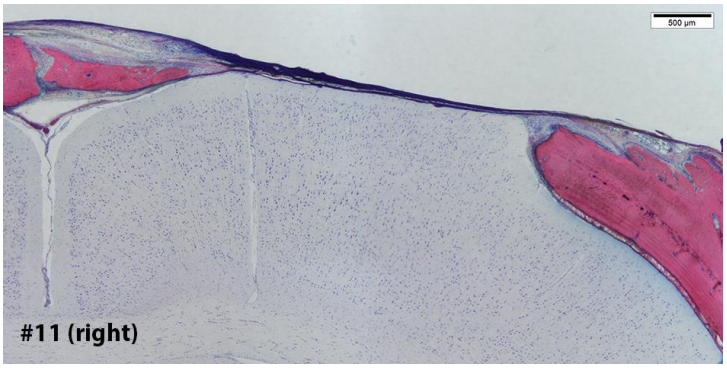

Figure 28: Calvarial defect of the empty defect without treatment. Note the very low defect closure ranging in this defect. (GE- stained, MMA-embedded thick-sections of the coronary plane through the defect center; for easier comparison of the defects the midline is always shown at left side of the picture, images of right-sided defect are mirrored, # = animal #, bar 500 µm)

5 Discussion

In this study, the effects on bone healing of sorted hBMSCs based on their Runx2/Sox9 ratio was investigated. Based on in vitro experiments, the hypothesis was that the sorted cells lead to more newly formed bone during bone healing of calvarial defects in nude rats than unsorted cells.

After four weeks all animals were at an advanced state of defect closure. The fact that the newly formed bone was still relatively thin and not yet reaching the original thickness of the calvarial bone shows that the defect closure was not yet finished. This is supported by the degree of vascularization of the new bone which is still higher than in the adjacent non-defect area. In approx. 35% of the samples membrane remnants could still be detected in the histological analysis which supports the assumption of ongoing formation and remodeling.

These findings are supported by the results of the fluorochrome marker Xylenol Orange (XO) showing red-orange marked lines not only in the periphery but also in the center of the defect. The red fluorescence line is caused by binding of the bone-seeking dye (XO) on Ca-ions in the matrix during new bone formation and shows the bone formation and remodeling at timepoint three weeks post OP. This means defect closure was already advanced at an early time point. New bone was formed without cartilaginous precursor tissue which characterizes the intra-membranous osteogenesis typical for calvarial bone.

However, the results of the CT evaluation showed no differences between sorted or unsorted cells. Interestingly, in the defects with membrane only more new bone was formed than in defects with membranes and cells. However, this was not statistically significant. The same result was observed for the defect closure in the histological examination.

Hence, these results did not support our hypothesis, that hBMSCs sorted based on their Runx2 to Sox9 ratio lead to more newly formed bone than unsorted cells in calvarial defects in nude rats. Even more, seeded cells had a negative impact on the amount of newly bone formed compared with the membrane only group. This is in contrast to previous publications such as Suenaga *et al*, who demonstrated that in nude rats hBMSCs spheroids implanted in calvarial defects lead to significantly better

bone regeneration than β-tricalcium phosphate (β-TCP) granules or a combination of hBMSCs and β-TCP. The hBMSCs spheroids were generated without the use of artificial materials or scaffolds.[29] Significantly better bone healing was also reported by Agacayak *et al* in rat calvarial defects treated with rat MSCs and platelet rich plasma (PRP) combined with synthetic biphasic calcium phosphate (BCP). This treatment showed the best healing compared to BCP alone, BCP plus PRP and BCP plus MSCs. With the combination of BCP plus MSCs the second-best healing was observed.[30] Thus, in this study it was shown that both MSCs and PRP played a crucial role in improving bone healing and lead to a better healing of the defects. However, in our study the defect closure analyzed by CT and histologically show that neither the sorted nor the unsorted cells have an impact on bone healing.

The above mentioned difference between the control group and the two groups with cells is even more obvious after two weeks. It is noticeable that less new bone was formed in group A and B compared to group C in the first two weeks after surgery. In the period between two and four weeks, approximately the same amount of new bone volume was formed in all three groups and the initially reduced bone formation in group A and B could be (partly) regained.

Based on this observation it can be hypothesized that the sorted and unsorted hBMSCs (group A and B) initially impair bone healing. If the cells are no longer present in the defect after two weeks, these defects can heal with the same amount of newly formed bone as the defects of the control group (group C). One possible explanation for this impairment could be an inflammation reaction against the cells. This could lead to an early degradation of the cells as well as the membrane. After degradation of the cells the bone ingrowth could start.

Nude rats should actually not trigger an inflammation reaction on human cells by their T-cell deficiency. This is the result of only a rudimentary thymic tissue.[31] However, this cannot be ruled out, since nude rats can develop T-like cells with increasing age.[32] In the study of Suenaga *et al* younger (seven compared to thirteen to seventeen week old used in this study) nude rats were used as recipient animals for the implantation of hBMSCs.[29]

Nevertheless, the innate immune system could be activated by the hBMSCs, this could lead to an inflammation with activity of phagocytes such as macrophages and

neutrophils. Furthermore, it is known that athymic rats have an increased activity of natural killer (NK) cells.[33, 34] Various authors describe, that NK cells play a major role in rejection of xenografts.[35–38] Thus, in this study the NK cells could also be responsible for a rejection of the hBMSCs used as a xenograft. Further studies would be needed to determine the exact role of NK cells in this model.

Based on the white blood cell count it cannot be concluded that the surgery led to a systemic inflammation. Therefore, at least two weeks after surgery, no systemic response to the membrane and cells was detectable. Nevertheless, a systemic inflammation may have occurred at a more recent time so that no changes in the blood value could be observed at the time of two weeks after surgery. Therefore, blood values of especially earlier time points would be needed.

To be able to prove this, a study with a shorter observation period could be performed, to determine histologically the period during which the cells are detectable in the defect and whether they trigger an inflammation.

Interestingly, most of the animals of the control group could largely bridge the defect. This reflects a high healing capacity of this animal species and shows the positive biological properties of the collagen membrane. The membrane itself appears to have a positive effect on bone healing, since in this study four out of five defects of the control group (group C) were mostly completely closed and these five millimeter defects are considered to be of critical size (see below for more details on critical size defect). Brunel *et al* and Song *et al* reported similar results. In their studies calvarial defects in rats filled with different collagen membranes healed better than empty defects.[39, 40] Based on the histological assessment, the membrane in group C seem to serve as a guiding structure. Bone ingrowth can take place along this path. Histologically it was shown that the intrinsic characteristics of the membrane facilitated bone formation directly on its surface (osteoconduction), and led also to partly incorporation (osteointegration). The low grade of both osteonecrosis and inflammation of adjacent soft tissue characterizes the high tissue compatibility of the membrane.

The membrane used in this study was a chemically non-crosslinked collagen I scaffold. Schmidt *et al* demonstrated in vitro that hMSCs seeded on the same collagen I membrane used in our study differentiated in osteogenic medium into

osteogenic lineage. This was shown due to their calcium phosphate mineralization. Without osteogenic medium no calcification could be seen. Also the membrane alone without cells but in osteogenic medium showed no mineralization.[41] In this study, comparing to the empty defect, the scaffold seems to promote the formation of new bone *in vivo*. However, this data is definitely only preliminary due to the low number of animals.

In six out of 17 defects light pink acellular material was observed. Due to its structure, it was defined as membrane remnants. As known from the observation of Rahmanian-Schwarz *et al* this membrane has a high biocompatibility and completely degrades 42 days after subcutaneous implantation in a rat model. Already 21 days after implantation only small residues could be noticed. No signs of wound healing disorders or inflammatory reaction could be observed.[42] With an observation period of 28 days in the available study these results match with the findings of Rahmanian-Schwarz *et al*. However, it would be an advantageous if further data on the degradation of the membrane in the calvarial defect model would be available. For this, the membranes without cells should be inserted into a calvarial defect and histological examinations should be carried out at earlier time points.

The surgery method was chosen based on descriptions by Spicer *et al* [20] and Cooper, Mooney *et al* .[43] Although it was not possible to drill all defects symmetrically round, this should not affect the calculation of the results. Through the post-surgery CT, the bone already present in the defect was excluded for further calculations.

Various authors describe that the dura plays an important role in the healing of calvarial bone defects.[20, 43, 44] Hobar *et al* demonstrated in guinea pigs that defects, filled with autologous bone, healed much better with greater osteoblastic numbers and osteoid activity when the dura was preserved compared to defects where the dura was resected. This observation was made both in immature and in mature animals.[45] Wang and Glimcher showed that the osteoblasts involved in calvarial bone defect healing were initially derived from undifferentiated MSCs of the dura.[46] In addition, it is hypothesized that the cerebrospinal fluid, which penetrates into the defects with an injury to the dura mater, could reduce or prevent the ossification. In summary, the dura mater plays an important role in healing of calvarial defects. Therefore, the goal of the surgical procedure was to avoid damage to the dura mater.

However, in three defects, the dura was injured, causing holes in the dura of about one Millimeter. In these defects, the smallest bone volume could be observed after four weeks compared to the other animals from the respective group. This difference was even more pronounced at two weeks. Thus, these results also show that the dura has a decisive influence on the healing of rat calvarial bone defects. If the defects with an injured dura mater are excluded from the evaluation, the differences between the groups increase, most likely reaching statistical significance.

Furthermore it is possible that in addition to the macroscopically visible dura mater defects, other non-visible lesions of the dura mater have been created which negatively affect healing. This could be the case, for example, when lifting the bone piece from the defect. Adhesions of the endost with the dura mater could be the cause in this case. The presence of non-visible dura mater defects could be a reason for the uneven distribution of the results in each group. In order to prevent the injuries of the dura mater, it would be possible to change the surgery method. There are perforators (Acra-Cut®, USA) available specially designed for perforating the cranium. The perforators can be connected to an ANSPACH® high speed electric system (DePuy Synthes, Switzerland). These instruments are commonly used in neurosurgery to perforate the cranium. In contrast to the trephine technique, the perforator is designed to automatically disengage once perforation is accomplished and when pressure is removed from the drill point. In consequence, no dura mater and brain injuries should be observed. We tried this method beforehand in a cadaver study but unfortunately the thickness of the rat skull is not thick enough. A minimum thickness of two mm is specified by the manufacturer for the five mm perforator.

Schmitz and Hollinger first defined in 1986 the critical size defect as “the smallest size intraosseous wound in a particular bone and species of animal that will not heal spontaneously during the lifetime of the animal”[47]. The critical size depends on the animal species, age, size and surgical technic (suturing the periosteum or not, dura mater preservation or injury). Bosch *et al* evaluated the critical size defect in the craniofacial region in five to six months old Wistar rats and defined a five mm calvarial defect as a critical size bone defect which heals by fibrous connective tissue formation. None of the untreated defects healed in this study and only connective tissue was present in the defects after twelve months.[22] Although we used younger animals in our study, they were also skeletally mature. Preliminary data of the

additional operated empty defect (animal # 11, right defect) showed that much less new bone was formed in this defect than in all other defects of group A, B and C. Even if this is only a single defect, it can be assumed that our defects were critical size defects. To support this hypothesis, it would be useful to have further data of more empty defects.

To avoid stress for the animal the rats have been accustomed to being handled and to any equipment used about four weeks prior to surgery. Based on the score and the weights it can be assumed that the burden of the animals is higher during the first week after surgery compared to the weeks two to four post op. However, the animals recovered very well and after one week post-surgery they all gained weight again. Over all the burden of the animals can be classified as moderate during the first week after surgery and as low from the second week on.

The limitations of this study are the small number of animals per group which were operated. In addition, the numbers of animals per group were unequal.

In order to achieve a statistical significance with the present non-normal distribution of the results, 17 defects per group would be required to determine after two weeks a difference with a probability of 80%. For a 90% probability, 22 defects would be needed. Since the difference was even lower after four weeks, even more defects per group would be needed at this time for a statistical significance. However, the clinical relevance of such data is questionable. With all the effort required for the cell sorting, a clear effect would be required. Since very clear differences in the groups have been shown in the *in vitro* experiments, the aim of this study was to prove this *in vivo*. If the *in vivo* study had shown similar results as the *in vitro* study, the group size would have been sufficient and a clear clinical relevance could be derived from these data.

A further limit of the study was the use of only one bone marrow donor. To generate more meaningful data, it would be necessary to investigate stem cells from different donors to rule out donor dependent effects.

One potential limitation of the study in the histological examination is the use of only one slice per defect for the histological analysis. In addition, the slice represents only a small part of the defect. Thus, changes like for example a possible dura mater injury, cannot be detected in a single histological slice if the injuries are not located in the incision plane but more rostral or caudal. Moreover, the histological examination

was only semi-quantitatively graded, additionally defect closure was estimated without absolute measurement of new formed bone. However, quantitative measurement by histomorphometry was not considered to be of additional value since the CT results could be used to calculate precise values of newly formed bone.

To investigate why the defects filled with sorted as well as unsorted cells on a membrane did not have an effect on bone healing compared to defects filled with only the membrane further studies are necessary. To be able to identify an inflammatory or immune reaction, histology data from earlier times would be necessary. Seven to ten days after surgery could be an appropriate time to detect macrophages histologically for example, since at this time the macrophages should be predominant in the tissue, as various authors described.[48–51]

In addition, more data regarding the healing of empty defects would also aim interpretation. This would be useful to prove the hypothesis that the membrane alone has a positive influence on bone healing. It would also be interesting to see whether two empty defects in the same animal show a similar healing or whether there are already differences within the animals.

Another point that could have had an influence is the cell culture procedure. Only the sorted cells were induced in osteogenic medium for one week whereas the unsorted cells were only cultured in growth medium. This was done in order to be able to compare the data with other studies, since normally uninduced cells are used. However, the induction of the sorted cells was necessary to be able to sort the cells afterwards. If the sorted cells had a markedly positive effect on the amount of the new bone formed, further studies would have been necessary. For example, a comparison between unsorted and sorted cells, both previously induced in osteogenic medium.

Conclusion:

In summary, the hypothesis that hBMSCs sorted based on their Runx2 to Sox9 ratio lead to more newly formed bone than unsorted cells in calvarial defects in nude rats could not be confirmed in the present study. In the defects with membrane only more new bone was formed than in defects with membranes and sorted or unsorted cells.

Nevertheless, neither in the CT nor in the histological analysis significant differences could be found. Further studies are needed to determine how long the cells are present in the defect and how they hinder bone healing.

The membrane itself appears to have positive effects on bone healing in terms of osteoconduction and osteointegration, if it is assumed that these five mm defects are critical size defects. However, a larger number of defects with membrane only and a comparison to empty defects would be necessary.

Funded:

The study was funded by AO CMF.

6 References

1. Janicki P, Schmidmaier G: What should be the characteristics of the ideal bone graft substitute? Combining scaffolds with growth factors and/or stem cells. *Injury* 2011;42 Suppl 2:S77-81.
2. Campana V, Milano G, Pagano E, et al.: Bone substitutes in orthopaedic surgery: From basic science to clinical practice. *Journal of materials science. Materials in medicine* 2014;25:2445–61.
3. Kolk A, Handschel J, Drescher W, et al.: Current trends and future perspectives of bone substitute materials - from space holders to innovative biomaterials. *Journal of cranio-maxillo-facial surgery official publication of the European Association for Cranio-Maxillo-Facial Surgery* 2012;40:706–18.
4. Bhatt RA, Rozental TD: Bone graft substitutes. *Hand clinics* 2012;28:457–68.
5. Finkemeier CG: Bone-Grafting and Bone-Graft Substitutes. *The Journal of Bone and Joint Surgery-American Volume* 2002;84:454–64.
6. Giannoudis PV, Dinopoulos H, Tsiridis E: Bone substitutes: An update. *Injury* 2005;36 Suppl 3:S20-7.
7. Wang X, Li G, Guo J, et al.: Hybrid composites of mesenchymal stem cell sheets, hydroxyapatite, and platelet-rich fibrin granules for bone regeneration in a rabbit calvarial critical-size defect model. *Experimental and therapeutic medicine* 2017;13:1891–9.
8. Nandi SK, Roy S, Mukherjee P, et al.: Orthopaedic applications of bone graft & graft substitutes: A review. *The Indian journal of medical research* 2010;132:15–30.
9. Laurencin C, Khan Y, El-Amin SF: Bone graft substitutes. *Expert review of medical devices* 2006;3:49–57.
10. Watt FM, Hogan BL: Out of Eden: Stem cells and their niches. *Science (New York, N.Y.)* 2000;287:1427–30.
11. Bethesda MD: *NIH Stem Cell Information Home Page: In Stem Cell Information [World Wide Web site]*. Available at: https://stemcells.nih.gov/info/basics.htm, 2016 [accessed 10.08.2017].
12. Maniar HH, Tawari AA, Suk M, et al.: The Current Role of Stem Cells in Orthopaedic Surgery. *Malaysian orthopaedic journal* 2015;9:1–7.

13. Ullah I, Subbarao RB, Rho GJ: Human mesenchymal stem cells - current trends and future prospective. *Bioscience reports* 2015;35.
14. Garg P, Mazur MM, Buck AC, et al.: Prospective Review of Mesenchymal Stem Cells Differentiation into Osteoblasts. *Orthopaedic surgery* 2017;9:13–9.
15. Li B, Menzel U, Loebel C, et al.: Monitoring live human mesenchymal stromal cell differentiation and subsequent selection using fluorescent RNA-based probes. *Scientific reports* 2016;6:26014.
16. Lefebvre V, Smits P: Transcriptional control of chondrocyte fate and differentiation. *Birth defects research. Part C, Embryo today reviews* 2005;75:200–12.
17. Bruderer M, Richards RG, Alini M, et al.: Role and regulation of RUNX2 in osteogenesis. *European cells & materials* 2014;28:269–86.
18. Loebel C, Czekanska EM, Bruderer M, et al.: In vitro osteogenic potential of human mesenchymal stem cells is predicted by Runx2/Sox9 ratio. *Tissue engineering. Part A* 2015;21:115–23.
19. Lahm H, Doppler S, Dressen M, et al.: Live fluorescent RNA-based detection of pluripotency gene expression in embryonic and induced pluripotent stem cells of different species. *Stem cells (Dayton, Ohio)* 2015;33:392–402.
20. Spicer PP, Kretlow JD, Young S, et al.: Evaluation of bone regeneration using the rat critical size calvarial defect. *Nature protocols* 2012;7:1918–29.
21. Gomes PS, Fernandes MH: Rodent models in bone-related research: The relevance of calvarial defects in the assessment of bone regeneration strategies. *Laboratory animals* 2011;45:14–24.
22. Bosch C, Melsen B, Vargervik K: Importance of the critical-size bone defect in testing bone-regenerating materials. *The Journal of craniofacial surgery* 1998;9:310–6.
23. Sawyer AA, Song SJ, Susanto E, et al.: The stimulation of healing within a rat calvarial defect by mPCL-TCP/collagen scaffolds loaded with rhBMP-2. *Biomaterials* 2009;30:2479–88.
24. Charles River: *RNU Rat* | *Nude Rats* | *Charles River*. Available at: http://www.criver.com/products-services/basic-research/find-a-model/rnu-rat, 2017 [accessed 23.06.2017].

25. Charles River: *PCR Infectious Agent Testing | Charles River*. Available at: http://www.criver.com/products-services/basic-research/health-monitoring-diagnostic-services/pria, 2017 [accessed 10.08.2017].
26. Bara JJ, Herrmann M, Menzel U, et al.: Three-dimensional culture and characterization of mononuclear cells from human bone marrow. *Cytotherapy* 2015;17:458–72.
27. Rahn BA, Perren SM: Xylenol orange, a fluorochrome useful in polychrome sequential labeling of calcifying tissues. *Stain Technology* 1971;46:125–9.
28. Bani Ismail Z, Abu Abeeleh M, Alzaben KR, et al.: Effects of experimental acute myocardial infarction on blood cell counts and plasma biochemical values in a nude rat model (Crl:NIH-Fox1RNU). *Comp Clin Pathol* 2009;18:433–7.
29. Suenaga H, Furukawa KS, Suzuki Y, et al.: Bone regeneration in calvarial defects in a rat model by implantation of human bone marrow-derived mesenchymal stromal cell spheroids. *Journal of materials science. Materials in medicine* 2015;26:254.
30. Agacayak S, Gulsun B, Ucan MC, et al.: Effects of mesenchymal stem cells in critical size bone defect. *European review for medical and pharmacological sciences* 2012;16:679–86.
31. Vos JG, Berkvens JM, Kruijt BC: The athymic nude rat. *Clinical immunology and immunopathology* 1980;15:213–28.
32. Rolstad B: The athymic nude rat: An animal experimental model to reveal novel aspects of innate immune responses? *Immunological reviews* 2001;184:136–44.
33. Jong WH de, Steerenberg PA, Ursem PS, et al.: The athymic nude rat. III. Natural cell-mediated cytotoxicity. *Clinical immunology and immunopathology* 1980;17:163–72.
34. Reynolds CW, Timonen TT, Holden HT, et al.: Natural killer cell activity in the rat. Analysis of effector cell morphology and effects of interferon on natural killer cell function in the athymic (nude) rat. *European journal of immunology* 1982;12:577–82.
35. Lin Y, Vandeputte M, Waer M: Natural killer cell- and macrophage-mediated rejection of concordant xenografts in the absence of T and B cell responses. *Journal of immunology (Baltimore, Md. 1950)* 1997;158:5658–67.
36. Kawahara T, Douglas DN, Lewis J, et al.: Critical role of natural killer cells in the rejection of human hepatocytes after xenotransplantation into immunodeficient

mice. *Transplant international official journal of the European Society for Organ Transplantation* 2010;23:934–43.

37. Lin M-L, Zhan Y, Nutt SL, et al.: NK cells promote peritoneal xenograft rejection through an IFN-gamma-dependent mechanism. *Xenotransplantation* 2006;13:536–46.
38. Manilay JO, Sykes M: Natural killer cells and their role in graft rejection. *Current opinion in immunology* 1998;10:532–8.
39. Brunel G, Piantoni P, Elharar F, et al.: Regeneration of rat calvarial defects using a bioabsorbable membrane technique: influence of collagen cross-linking. *Journal of periodontology* 1996;67:1342–8.
40. Song KY, Um YJ, Jung UW, et al.: The Effects of Collagen Membrane Coated with PLGA on Bone Regeneration in Rat Calvarial Defects. *KEM* 2007;342-343:357–60.
41. Schmidt T, Stachon S, Mack A, et al.: Evaluation of a thin and mechanically stable collagen cell carrier. *Tissue engineering. Part C, Methods* 2011;17:1161–70.
42. Rahmanian-Schwarz A, Held M, Knoeller T, et al.: In vivo biocompatibility and biodegradation of a novel thin and mechanically stable collagen scaffold. *Journal of biomedical materials research. Part A* 2014;102:1173–9.
43. Cooper GM, Mooney MP, Gosain AK, et al.: Testing the critical size in calvarial bone defects: Revisiting the concept of a critical-size defect. *Plastic and reconstructive surgery* 2010;125:1685–92.
44. Hobar PC, Schreiber JS, McCarthy JG, et al.: The role of the dura in cranial bone regeneration in the immature animal. *Plastic and reconstructive surgery* 1993;92:405–10.
45. Hobar PC, Masson JA, Wilson R, et al.: The importance of the dura in craniofacial surgery. *Plastic and reconstructive surgery* 1996;98:217–25.
46. Wang J, Glimcher MJ: Characterization of matrix-induced osteogenesis in rat calvarial bone defects: II. Origins of bone-forming cells. *Calcified tissue international* 1999;65:486–93.
47. Schmitz JP, Hollinger JO: The critical size defect as an experimental model for craniomandibulofacial nonunions. *Clinical orthopaedics and related research* 1986:299–308.
48. Taketo MM: Reflections on the spread of metastasis to cancer prevention. *Cancer prevention research (Philadelphia, Pa.)* 2011;4:324–8.

49. Koh TJ, DiPietro LA: Inflammation and wound healing: the role of the macrophage. *Expert reviews in molecular medicine* 2011;13:e23.
50. Serhan CN, Petasis NA: Resolvins and protectins in inflammation resolution. *Chemical reviews* 2011;111:5922–43.
51. Nauta TD, van Hinsbergh VWM, Koolwijk P: Hypoxic signaling during tissue repair and regenerative medicine. *International journal of molecular sciences* 2014;15:19791–815.

7 Attachments

Group allocation

Table 10: Group allocation, *: This animal died during anesthesia before surgery

Animal #	Left defect filled with group	Right defect filled with group
0	NA*	NA*
1	B	C
2	C	B
3	C	B
4	A	B
5	A	C
6	B	A
7	C	A
8	A	B
9	B	A
10	C	A
11	C	empty

Health report:

charles river

HEALTH REPORT

Printed on : 11/10/2016
Page : 1

AO FORSCHUNGSINSITUT **12** **NUDE RAT** **DN N° : EEW29863**

Unit N° : **18** Specie : **RAT** Health Status : **SOPF**

Summary Item	Primary Assay	Primary Lab	Most Recent Year Week*	Most Recent Positive / Tested	Past 18 Months Positive / Tested
Viruses					
RPV	a e MFIA	RADS EU	2016-24	0 / 4	0 / 28
RMV	a e MFIA	RADS EU	2016-24	0 / 4	0 / 28
H1	a e MFIA	RADS EU	2016-24	0 / 4	0 / 28
KRV	a e MFIA	RADS EU	2016-24	0 / 4	0 / 28
TMEV (GDVII)	a e MFIA	RADS EU	2016-24	0 / 4	0 / 28
SDAV	a e MFIA	RADS EU	2016-24	0 / 4	0 / 28
REO	a e MFIA	RADS EU	2016-24	0 / 4	0 / 28
SEND	a e MFIA	RADS EU	2016-24	0 / 4	0 / 28
PVM	a e MFIA	RADS EU	2016-24	0 / 4	0 / 28
MAV	a e MFIA	RADS EU	2016-24	0 / 4	0 / 28
LCMV	a e MFIA	RADS EU	2016-24	0 / 4	0 / 28
HANT	a e MFIA	RADS EU	2016-24	0 / 4	0 / 28
Mycoplasma					
M. pulmonis	a e MFIA	RADS EU	2016-24	0 / 4	0 / 28
Bacteria					
Pneumocystis spp.	a e MFIA	RADS EU	2016-24	0 / 8	0 / 56
Tyzzer's Disease	a e Exam	RADS EU	2016-24	0 / 8	0 / 56
B. bronchiseptica	a e Culture	RADS EU	2016-24	0 / 8	0 / 56
C. kutscheri	a e Culture	RADS EU	2016-35	0 / 4	0 / 106
P. pneumotropica	a e Culture	RADS EU	2016-35	0 / 4	0 / 106
P. multocida	a e Culture	RADS EU	2016-35	0 / 4	0 / 106
Salmonella spp.	a e Culture	RADS EU	2016-24	0 / 8	0 / 56
S. moniliformis	a e PCR	RADS EU	2016-24	0 / 8	0 / 56
Beta Strep. sp.	a e Culture	RADS EU	2016-35	0 / 4	0 / 106
Strep. pneumoniae	a e Culture	RADS EU	2016-35	0 / 4	0 / 106
H. hepaticus	a e PCR	RADS EU	2016-24	0 / 4	0 / 28
H. bilis	a e PCR	RADS EU	2016-24	0 / 4	0 / 28
Helicobacter sp.	a e PCR	RADS EU	2016-24	0 / 4	0 / 28
Staph. aureus	a d Culture	RADS EU	2016-35	0 / 4	0 / 106
P. aeruginosa	a d Culture	RADS EU	2016-35	0 / 4	0 / 106
K. pneumoniae	a d Culture	RADS EU	2016-35	0 / 4	0 / 106
K. oxytoca	a d Culture	RADS EU	2016-35	0 / 4	0 / 106
P. mirabilis	a d Culture	RADS EU	2016-35	0 / 4	0 / 106
CAR Bacillus	a e MFIA	RADS EU	2016-24	0 / 4	0 / 28
Parasites					
Ectoparasites	a e Exam	RADS EU	2016-24	0 / 8	0 / 56
E. cuniculi	a e MFIA	RADS EU	2016-24	0 / 4	0 / 28
Pathogenic Protozoa	a e Exam	RADS EU	2016-24	0 / 8	0 / 56
Other Protozoa	a e Exam	RADS EU	2016-24	0 / 8	0 / 56
Helminths	a e Exam	RADS EU	2016-24	0 / 8	0 / 56
Lesions observed					
Gross Exam	b g Exam	RADS EU	2016-24	0 / 8	0 / 56

Legend :

Legend:
RADS EU = Research Animal Diagnostic Services Europe Lyon, France
RADS US = Research Animal Diagnostic Services United States Wilmington
, Massachusetts

COLONY POLICY FOR POSITIVE RESULT: a = immediate termination; b = pla

Figure 29: Health report with all tested infectious agents; page 1/2

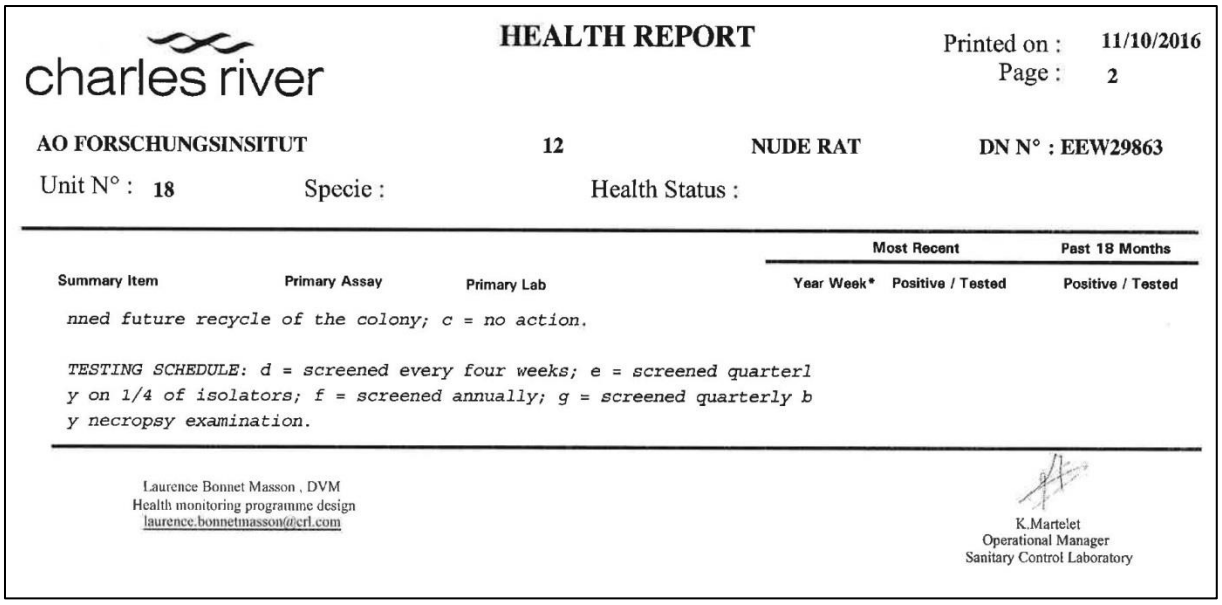

charles river

HEALTH REPORT

Printed on : 11/10/2016
Page : 2

AO FORSCHUNGSINSITUT **12** **NUDE RAT** **DN N° : EEW29863**

Unit N° : **18** Specie : Health Status :

Summary Item	Primary Assay	Primary Lab	Most Recent Year Week*	Most Recent Positive / Tested	Past 18 Months Positive / Tested

nned future recycle of the colony; c = no action.

TESTING SCHEDULE: d = screened every four weeks; e = screened quarterl y on 1/4 of isolators; f = screened annually; g = screened quarterly b y necropsy examination.

Laurence Bonnet Masson , DVM
Health monitoring programme design
laurence.bonnetmasson@crl.com

K.Martelet
Operational Manager
Sanitary Control Laboratory

Figure 30: Health report with all tested infectious agents; page 2/2

Health monitoring: PCR Rodent Infectious Agent Test

Rat Panels — Direct Animal Sampling

	Enteric	Prevalent	Fecal	Surveillance	Surveillance Plus	FELASA Basic (3-Month)	FELASA Complete (Annual)	Bacteria-Only
Viruses								
Rat parvoviruses (H-1, KRV, RPV, RMV)	•	•	•	•	•	•	•	
Rat coronavirus (RCV, SDAV)	•	•	•	•	•	•	•	
Rat theilovirus (RTV)	•	•	•	•	•	•	•	
Adenovirus type 1 & 2 (MAV-1 & MAV-2)			•	•	•		•	
Reovirus type 1, 2, 3, 4			•	•	•		•	
Pneumonia virus of mice					•	•	•	
Sendai virus					•		•	
Seoul (hantavirus)			•	•	•		•	
New World hantavirus*								
Bacteria								
Helicobacter	•	•	•	•	•	•	•	•
Mycoplasma pulmonis					•	•	•	•
Streptobacillus moniliformis			•	•	•		•	•
Pasteurella pneumotropica (Heyl & Jawetz)	•	•	•	•	•	•	•	•
Clostridium piliforme			•	•	•	•	•	•
CAR *Bacillus*					•		•	•
Pseudomonas aeruginosa				•	•			•
Salmonella			•	•	•		•	•
Campylobacter			•	•	•			•
Bordetella bronchiseptica					•			•
Corynebacterium kutscheri			•	•	•			•
Staphylococcus aureus			•	•	•			•
Streptococcus pneumoniae			•	•	•	•	•	•
Klebsiella pneumoniae			•	•	•			•
Klebsiella oxytoca			•	•	•			•
Beta hemolytic *Streptococcus* group A					•	•	•	•
Beta hemolytic *Streptococcus* group B			•	•	•	•	•	•
Beta hemolytic *Streptococcus* group C			•	•	•	•	•	•
Beta hemolytic *Streptococcus* group G			•	•	•	•	•	•
Proteus mirabilis			•	•	•			•
*Leptospira**								
Parasites/Protozoa/Fungi								
Fur mites *(Myobia, Myocoptes, Radfordia)*		•		•	•	•	•	
Pinworms *(Aspiculuris, Syphacia)*	•	•		•	•	•	•	
Giardia			•	•	•	•	•	
Spironucleus muris		•	•	•	•	•	•	
Cryptosporidium			•	•	•	•	•	
Entamoeba		•	•	•	•	•	•	
Pneumocystis		•			•		•	

** Available as a wild rodent add-on*

Figure 31: Surveillance PRIA: List of all agents [25]

Micro computed tomography data:

Table 11: Bone volume

Group	Animal #	Side	Bone Volume [mm^3]					
			Individual			Average ± standard deviation		
			post OP	2 weeks	4 weeks	post OP	2 weeks	4 weeks
A	4	L	0.000	0.416	1.316	0	0.486 ± 0.197	1.798 ± 0.693
	5	L	0.000	0.348	1.179			
	6	R	0.000	0.477	2.770			
	7	R	0.000	0.389	1.361			
	8	L	0.000	0.407	1.586			
	9	R	0.000	0.878	2.576			
B	1	L	0.000	0.525	2.279	0	0.488 ± 0.192	1.860 ± 0.611
	3	R	0.000	0.515	1.528			
	4	R	0.000	0.341	2.053			
	6	L	0.000	0.573	1.930			
	8	R	0.000	0.210	0.824			
	9	L	0.000	0.764	2.544			
C	1	R	0.000	0.286	0.752	0	0.810 ± 0.458	2.362 ± 1.043
	3	L	0.000	1.069	3.044			
	5	R	0.000	0.957	2.307			
	7	L	0.000	1.351	3.489			
	11	L	0.000	0.385	2.220			
empty	11	R	0.000	0.172	0.656	NA	NA	NA

Micro computed tomography images post OP:

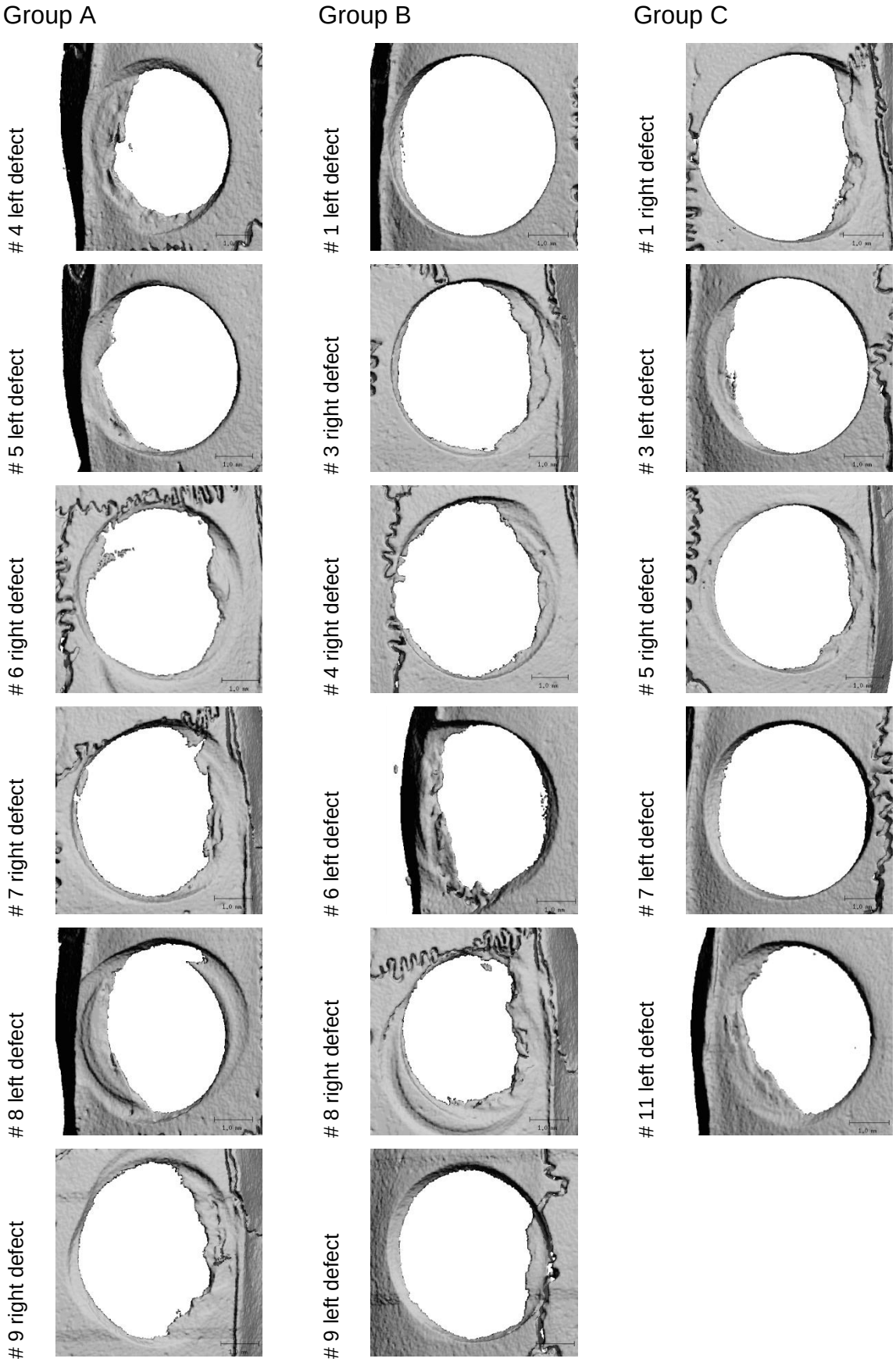

Figure 32: CT images post OP, rostral: always shown at top of the picture

Micro computed tomography images 2 weeks post OP

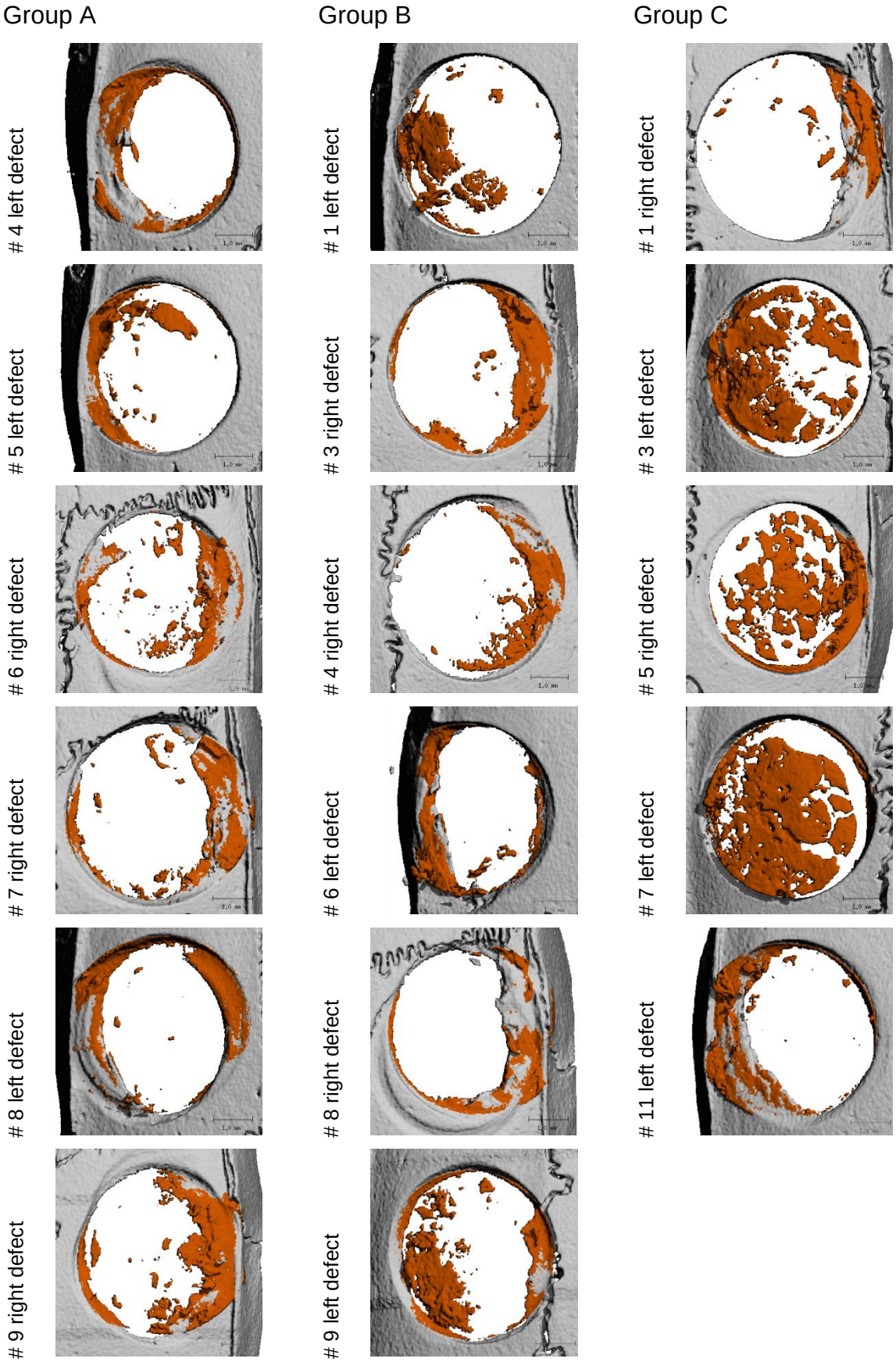

Figure 33: CT images 2 weeks post OP, rostral: always shown at top of the picture

Micro computed tomography images 4 weeks post OP

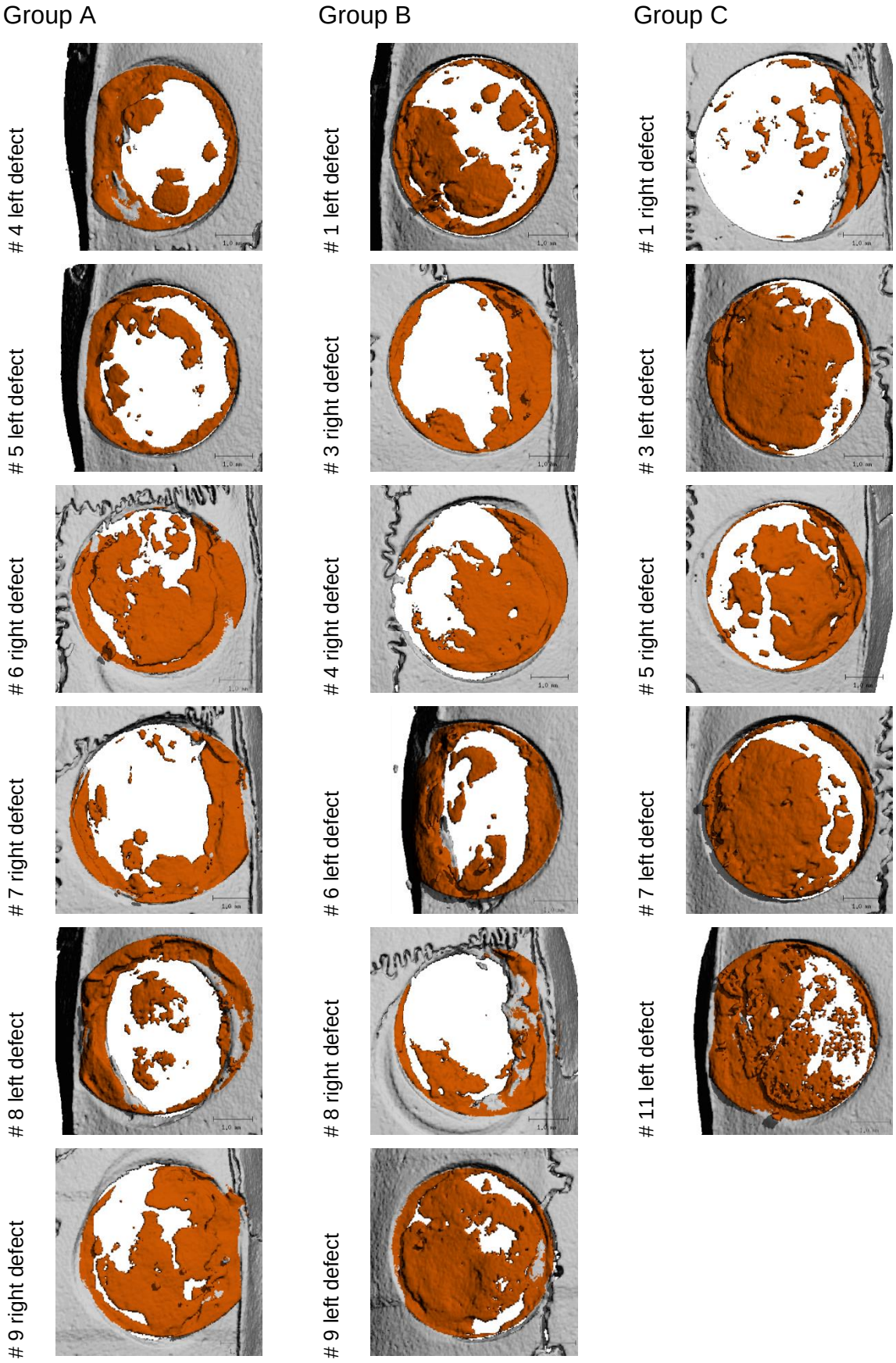

Figure 34: CT images 4 weeks post OP, rostral: always shown at top of the picture

Micro computed tomography image empty defect

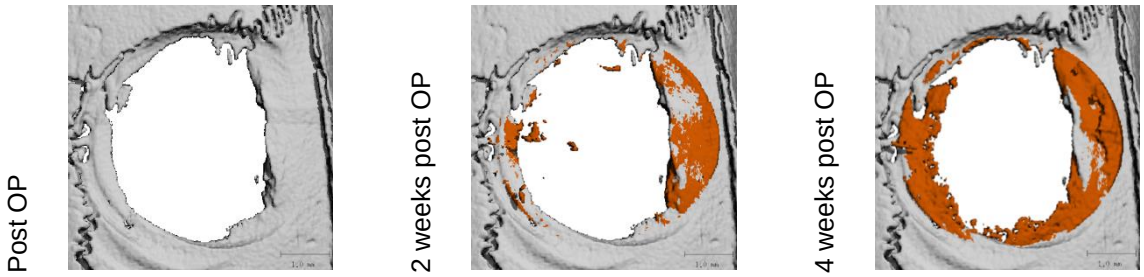

Figure 35: CT images empty defect (# 11 right defect), rostral: always shown at top of the picture

Histological analysis

Histological grading:

Table 12: Histological grading

Grade	Grading general	Grading defect closure
1	minimal	1-20 %
2	slight	-40 %
3	moderate	-60 %
4	marked	-80 %
5	massive	-100%

Table 13: Grading of metal remnants:

Grade	Grading metal remnants
0	not present
P	present

Table 14: Raw data table of the grading of histological findings (per animal, per group)

Group		A						B						C					Empty
Treatment		membrane + sorted MSCs						membrane + unsorted MSCs						membrane only					Empty
Location (L/R)		L	L	R	R	L	R	L	R	R	L	R	L	R	L	R	L	L	R
Animal No		4	5	6	7	8	9	1	3	4	6	8	9	1	3	5	7	11	11
Histo No (GE)		27217/18	27218/07	27219/12	27220/09	27221/14	27222/09	27215/12	27216/14	27217/13	27219/18	27221/08	27222/12	27215/5	27216/11	27218/05	27220/15	27227/12	27227/6
metal remnants	remarks										fascia								
	[0/P]	0	0	0	0	0	0	0	P	0	P	0	0	0	0	0	0	0	0
hemosiderin, soft tissue, near defect	remarks										subdural								
	[grade 1-5]	1	2	1	2	0	1	2	1	2	2	0	2	1	2	2	1	2	0
inflammation, lymphocytic, soft tissue	remarks										fascia								
	[grade 1-5]	0	0	0	0	0	0	0	0	0	1	0	0	0	0	0	0	0	0
inflammation, granulom., soft tissue	remarks		around membrane material				suture material				around metal				around membrane material		around hair	suture material	suture material
	[grade 1-5]	0	1	1	1	1	1	0	1	1	1	1	1	0	1	1	1	3	2
defect closure by new bone, in %, [estimated]	STDEV	34.8						37.3						17.9					
	mean [in %]	54.3						54.7						82.0					
	in %, [estimated]	21	55	95	15	45	95	98	20	75	45	5	85	50	90	90	90	90	5
defect closure by new bone [grade 1-5, see above %]	mean	3.2						3.2						4.6					1.0
	[grade 1-5]	2	3	5	1	3	5	5	1	4	3	1	5	3	5	5	5	5	1
thickness of new calvarial bone	mean	2.0						2.2						2.6					
	[grade 1-5]	2	3	3	1	1	2	3	2	2	2	1	3	1	3	3	3	3	0
vascularization, of new calvarial bone	mean	2.2						1.7						2.6					
	[grade 1-5]	1	3	4	0	2	3	2	2	2	1	0	3	1	3	3	3	3	0
necrosis, of new calvarial bone (empty lacunae)	mean	0.5						0.2						1.0					
	[grade 1-5]	2	0	0	0	1	0	0	0	0	0	1	0	2	2	0	1	0	0
brown finegranular material (degraded collagen membrane ?)	mean	1.7						1.5						2.6					
	[grade 1-5]	1	3	1	1	2	2	1	0	3	1	1	3	3	1	3	3	3	0
light pink, acellular material (membrane remnants)																			
	[grade 1-5]	-	3	1	-	-	-	1	-	-	-	-	2	-	2	3	2	-	-
Histo No (FL)		27217/17	27218/06	27219/11	27220/08	27221/15	27222/10	27215/13	27216/15	27217/14	27219/17	27221/07	27222/13	27215/6	27216/10	27218/06	27220/16	27227/11	27227/04
red FL signal (xylenol orange), periphery (filter set 25)	mean	1.8						1.7						1.6					
	[grade 1-5]	2	2	2	1	2	2	1	2	2	2	1	2	1	2	1	2	2	1
red FL signal (xylenol orange), central (filter set 25)	mean	0.8						1.0						1.4					
	[grade 1-5]	0	1	2	0	0	2	1	1	1	1	0	2	0	1	2	2	2	0

Statistical values:

Factor treatment (groups):

Table 15: Statistical values of the influence of the factor treatment (groups)

Parameter		Value	p-value
CT	Bone volume after 2 weeks	1.12	0.57
	Bone volume after 4 weeks	1.35	0.51
	Inferred bone growth	1.06	0.59
Histology	Defect closure	1.71	0.43
	Thickness	1.78	0.41
	Vascularization	2.28	0.32

Factor time:

Table 16: Statistical values of the influence of the factor time

Parameter	Chi	p
Bone volume measured with CT	21.144	<0.05
WBC values	5.85	=0.05

8 List of Abbreviations

BW	Bodyweight
CT	Computed tomography
EDTA	Ethylenediaminetetraacetic acid
ESCs	Embryonic stem cells
FACS	Fluorescence activated cell sorting
FL	Fluorescence
GE	Giemsa eosin
h	hour
HIV	Human immunodeficiency virus
kg	Kilogram
IVC	Individually ventilated cages
hBMSCs	Human bone marrow mesenchymal stem cells
mg	Milligram
ml	Milliliter
MMA	Methyl Methacrylate
MSCs	Mesenchymal stem cells
NaCl	Sodium chloride
OP	Operation
ROI	Region of interest
rpm	revolutions per minute
s.c.	subcutaneously
SD	Standard deviation
SPF	Specific pathogen free
VOI	Volume of interest
WBC	White blood cells
XO	Xylenol Orange
µCT	Micro computed tomography
#	Number

Acknowledgements

First, I am grateful for all the support I have received from Prof. Anton Fürst and for his excellent supervision of my thesis. I would like to thank Dr. med. vet. Stephan Zeiter and Prof. Martin Stoddart for giving me the opportunity to work on such an interesting project, the stimulating scientific discussions and for their ongoing support.

Special thanks to Dr. med. vet. Stephan Zeiter for the excellent supervision, practical and theoretical help and for his critical reading of the thesis.

Many thanks also to the team of the Preclinical Facility at the AO Research Institute Davos for their help, useful suggestions, the incredible teamwork and the friendly atmosphere; I am especially grateful to Dr. med. vet. Tanja Schmid for her support in developing the surgical procedure.

In addition, I would like to acknowledge the contribution of Ursula Eberli and Dr. med. Dominic Gehweiler for answering all my questions and their practical help with the microCT imaging and analysis.

I would also like to express my gratitude to Dr. med. vet. Dirk Nehrbass for his outstanding help with histological analysis and sharing his experience in histopathology with me.

Additionally, Dr. Volkher Scholz deserves a special mention for his help with the statistical analysis.

Finally, I am deeply grateful to my family for supporting me throughout my life and to Lydia for her ongoing support and understanding.

Curriculum Vitae

Name	Fabian Gieling
Geburtsdatum	05. September 1990
Geburtsort	Steinheim, Deutschland
Nationalität	deutsch, niederländisch

Schulausbildung

08/1997 – 07/2001	Grundschule am Paradies, Blomberg, Deutschland
08/2001 – 06/2010	Hermann-Vöchting-Gymnasium, Blomberg, Deutschland
18.06.2010	Abitur, Hermann-Vöchting-Gymnasium, Blomberg, Deutschland

Studium

10/2010 – 03/2016	Studium der Veterinärmedizin an der Stiftung Tierärztliche Hochschule Hannover, Deutschland
22.03.2016	Staatsexamen vet. med. Stiftung Tierärztliche Hochschule Hannover, Deutschland

Doktorat

02/2017 – 09/2017	Anfertigung der Dissertation unter der Leitung von Prof. Dr. med. vet. Anton Fürst am Departement für Pferde der Vetsuisse-Fakultät, Universität Zürich Direktor: Prof. Dr. med. vet. Anton Fürst

Fachrelevante Anstellungen

04/2016 – 08/2017	Doctoral Student, AO Research Institute, Davos, Schweiz
ab 09/2017	Junior Project Leader, AO Research Institute, Davos, Schweiz